

Supernova Hosts for Gamma-Ray Burst Jets: Dynamical Constraints

Christopher D. Matzner^{1,2}

¹Canadian Institute for Theoretical Astrophysics, University of Toronto

²Present address: Dept. of Astronomy and Astrophysics, University of Toronto, 60 St. George Street, Toronto, ON M5S 3H8, Canada

Received xxxx, 2002

ABSTRACT

I constrain a possible supernova origin for gamma-ray bursts by modeling the dynamical interaction between a relativistic jet and a stellar envelope surrounding it. The delay in observer's time introduced by the jet traversing the envelope should not be long compared to the duration of gamma-ray emission; also, the jet should not be swallowed by a spherical explosion it powers. The only stellar progenitors that comfortably satisfy these constraints, if one assumes that jets move ballistically within their host stars, are compact carbon-oxygen or helium post-Wolf-Rayet stars (type Ic or Ib supernovae); type II supernovae are ruled out. Notably, very massive stars do not appear capable of producing the observed bursts at any redshift unless the stellar envelope is stripped prior to collapse. The presence of a dense stellar wind places an upper limit on the Lorentz factor of the jet in the internal shock model; however, this constraint may be evaded if the wind is swept forward by a photon precursor. Shock breakout and cocoon blowout are considered individually; neither presents a likely source of precursors for cosmological GRBs.

These envelope constraints could conceivably be circumvented if jets are laterally pressure-confined while traversing the outer stellar envelope. If so, jets responsible for observed GRBs must either have been launched from a region several hundred kilometers wide, or have mixed with envelope material as they travel. A phase of pressure confinement and mixing would imprint correlations among jets that may explain observed GRB variability-luminosity and lag-luminosity correlations.

Key words: gamma rays: bursts, supernovae: general, shock waves, relativity

1 INTRODUCTION

There is presently a growing body of circumstantial evidence linking some long-duration gamma ray bursts (GRBs) with afterglows to the explosions of massive stars. Supernovae (SN) or supernova-like features have been identified in seven afterglows (Galama et al. 1998; Bloom et al. 1999; Reichart 1999; Turatto et al. 2000; Björnsson et al. 2001; Lazzati et al. 2001) although some of these could be light echoes from dust clouds (Esin & Blandford 2000). The afterglows of six other GRBs have been interpreted in terms of a wind-like ambient medium as expected around a massive star at the end of its life (Frail et al. 1999; Holland et al. 2001; Frail et al. 2000; Li & Chevalier 2001; Price et al. 2002). However these are often equally well explained by a collimated flow in a uniform medium. X-ray lines have been detected with moderate confidence in about half the afterglows for which they were investigated (Toshio & Daisuke 2000); however, the data analysis has been questioned (see Rutledge & Sako 2003). If real, these are most easily ex-

plained by dense material surrounding the burst engine, suggesting a stellar origin (e.g., Böttcher & Fryer 2001).

Frail et al. (2001) have recently derived beaming angles for a number of GRBs from observations of their afterglows. These authors derive gamma-ray energies reminiscent of supernovae: roughly 3×10^{50} erg for the observed lobes of GRBs. Similar results were reported by Panaitescu & Kumar (2001) and Freedman & Waxman (2001).

Clear evidence that GRBs occur very close to massive star formation would be almost as conclusive as a SN signature in an individual GRB. Several GRB afterglows show evidence for high column densities (980703 and 980329; Galama & Wijers 2001) or high local gas densities (000926 and 980519; Harrison et al. 2001, Wang et al. 2000), both of which connote star-forming regions. Likewise, the intrinsic extinction of GRB 000926 is characteristic of a galaxy disk (Price et al. 2001). Bloom, Kulkarni, & Djorgovski (2002) have shown that the observed locations within hosts imply a tight correlation between GRBs and stellar populations,

arXiv:astro-ph/0203085v2 6 Jul 2003

considered too tight (Bloom et al. 1999b) to be matched by merging neutron stars. Note however that the locations of merging neutron star pairs depends on their uncertain distribution of natal kicks.

If GRBs are a rare byproduct of star formation, rapidly star-forming galaxies should be over-represented as GRB hosts. In optical light host galaxies tend to look ordinary compared to contemporaries in the Hubble Deep Field, but [Ne III] and [O II] and infrared observations often indicate elevated star formation rates (Djorgovski et al. 2001). At least eight afterglows have been associated with starburst or interacting galaxies (Djorgovski et al. 2001; Frail et al. 2002; Chary, Becklin, & Armus 2002).

Although the association between long-duration GRBs and SNe is tentative (and applies only to the long-duration bursts for which afterglows are observed), the above evidence warrants a careful evaluation. There are two ways a SN can create a GRB. Colgate (1968) predicted that gamma rays might be produced in the very fastest, outermost ejecta of an ordinary supernova explosion. This proposal was recently revived by Matzner & McKee (2000) and Tan et al. (2001). These authors showed that the GRB (980425) most compellingly associated with a SN (1998bw) is likely to be the result of trans-relativistic SN ejecta colliding with a stellar wind (see also Matzner, Tan, & McKee 2001). In their model, as conjectured by Iwamoto et al. (1998), SN 1998bw was spherically symmetric or mildly asymmetric, and produced the GRB in an external shock. Scaled-up versions of this model could produce external shock GRBs, at the expense of vast amounts ($\sim 10^{54}$ erg) of energy in nonrelativistic ejecta.

In contrast, Sari & Piran (1995) have argued that most GRBs require internal emission (e.g., by internal shocks) within unsteady ultrarelativistic winds or jets, as originally suggested by Rees & Meszaros (1994). The arguments for internal emission are strongest for rapidly-fluctuating cosmological bursts with hard spectra, those least resembling GRB 980425; also, see Dermer & Mitman (1999) for arguments in support of external shocks. I shall assume for the purposes of this investigation that cosmological GRBs involve internal emission within optically thin, ultrarelativistic outflows. For this to result from a SN, a jet must emanate from a star’s core and pierce its envelope – shedding the baryons in its path – prior to producing the gamma rays observed at Earth. Such a jetlike explosion is the conventional model (e.g., MacFadyen & Woosley 1999) for a supernova origin of cosmological GRBs.

The goal of this paper will be to develop analytical models for the phase of this latter model in which a jet, already created by the stellar core, must traverse the envelope and shove aside material in its path. These models, which are complementary to numerical simulations (Aloy et al. 2000), are meant to elucidate under what conditions the hypothesis of a stellar origin is viable for the observed GRBs. In §§2 and 3 I assume that jets travel ballistically within their stars; this allows one to place strict constraints on stellar envelopes. In §6 this assumption is reconsidered. It is shown that a phase in which the jet is hot, pressure confined, and mixing with its environs would have interesting consequences.

1.1 Stellar Progenitors

Figure 1 sketches the typical masses and radii of the stellar GRB progenitor candidates considered in this paper. In general, those that retain an outer envelope (e.g., supergiants) have quite large radii ($R > 10 R_{\odot}$) at the time of core collapse, whereas those depleted in hydrogen due to winds or binary interaction (e.g., those that have been through a Wolf-Rayet phase) are quite compact ($R < 10 R_{\odot}$). Among post-Wolf-Rayet stars, those containing helium (“He Wolf-Rayets” on the plot) are less compact than their He-depleted peers (“C/O Wolf-Rayets”).

Very massive objects (VMOs) might have formed at high redshift due to the difficulty of cooling in the absence of metals and thus the large Jeans mass in primordial gas (Hartquist & Cameron 1977). VMOs may also form today in rare conditions. Those initially more massive than $\sim 250M_{\odot}$ die when their cores collapse to black holes, and are candidates for producing GRBs; Bond et al. (1984) discuss their evolution. Again, the pre-collapse radii of these stars depend on their mass loss. If present, their H envelope is quite diffuse (see Fryer et al. 2001). Otherwise the remaining convective core is very compact at the point of collapse. In addition to winds and binary mass transfer, VMOs may shed their envelopes in a super-Eddington phase during helium core contraction. Lone VMOs are thought to retain H envelopes if they are formed from sufficiently low-metallicity gas (although this is uncertain; Bond et al. 1984).

The “supranova” model of Vietri & Stella (1999) posits that a SN explosion produces a rapidly spinning neutron star massive enough to collapse after shedding its angular momentum (Baumgarte & Shapiro 1999) along with $\sim 10^{53}$ erg of rotational energy. The object collapses to a black hole with an accretion torus, firing a jet through the pulsar’s wind nebula and its sheath of stellar ejecta. Because of the short viscous times of such tori, this model is most appropriate for short GRBs rather than the long bursts for which there is evidence of a SN connection. Also, we will see in §3 that the expanding stellar ejecta would prevent the production of a GRB entirely, unless it has either become Thompson optically thin or has been cleared aside by the breakout of the pulsar wind nebula. The latter is possible in this model, because the pulsar spindown energy exceeds the typical kinetic energy of SN ejecta.

Fryer & Woosley (1998) and Zhang & Fryer (2001) discuss a scenario in which the stellar core collapse leading to a GRB results from the coalescence of a helium Wolf-Rayet star with a compact companion. Similarly, Fryer et al. (1999) argue that binary mergers are likely to dominate the production stars whose cores collapse to black holes accreting through a disk. Progenitors created in this fashion will typically be stripped of their outer envelopes, hence compact. However the stripped envelope poses a potential barrier to jet propagation, as in the supranova model, unless it is strictly confined to the equator of the system or has expanded to the point of being optically thin.

In sections 2.1 and 6.1 I examine the properties of stellar cores at the point of collapse. For this I shall assume that collapse sets in at the oxygen ignition temperature, $T_9 \equiv T/10^9$ K $\simeq 3.2$ (e.g., Bond et al. 1984).

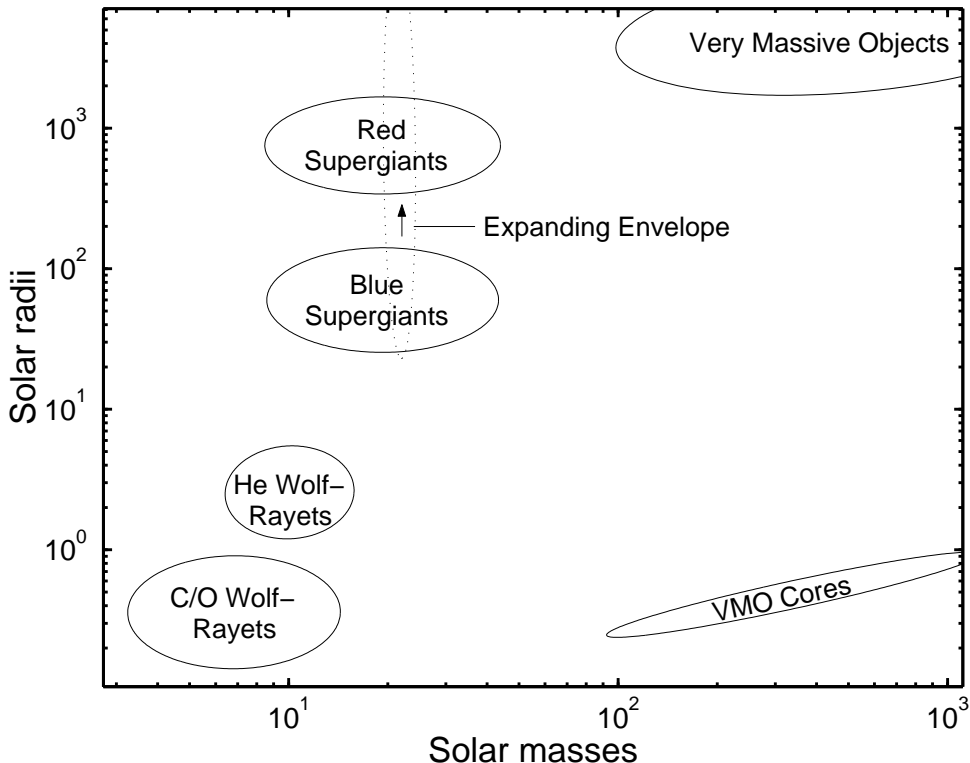


Figure 1. Schematic of the typical masses and radii of the stellar progenitors considered in this paper (§1.1). The plotted regions each represent several pre-supernova stellar models from the literature.

2 JETS WITHIN STARS AND STELLAR WINDS

Consider the progress of a relativistic jet outward from a star’s core through the stellar envelope. Schematically, three distinct regions develop: the propagating jet; the *head* of the jet, where jet material impacts the stellar envelope, and a *cocoon* consisting of shocked jet and shocked ambient material. These are familiar components from the theory of radio galaxies (Begelman & Cioffi 1989); see figure 2.

2.1 Presence of an uncollapsed envelope

Stellar envelopes pose a problem for the propagation of GRB jets only if they have not collapsed prior to the launching of the jet. The stellar envelope’s collapse timescale is greater (probably by a factor of at least a few) than its free-fall time t_{ff} . In figure 3 I compare stellar free-fall times with the intrinsic durations of GRBs for several possible redshifts. Only the very dense progenitors, the cores of very massive objects ($t_{\text{ff}} = 23(M_{\text{core}}/[100 M_{\odot}])^{1/4}$ s at oxygen ignition) and helium depleted post-Wolf-Rayet stars ($t_{\text{ff}} \gtrsim 50$ s) could plausibly collapse entirely in the durations of the longest GRBs, and then only at low redshift. In all other cases a stellar envelope remains to impede GRB jets.

2.2 Head Motion

For stellar core collapse to successfully produce a cosmological GRB, it must emit a jet that clears the stellar envelope from the observer’s line of sight to the core. This is

required if the jet is to achieve high Lorentz factors and if its internal shocks are to be unobscured by overlying material. This cannot occur if the Lorentz factor of the jet head, $\Gamma_h \equiv (1 - \beta_h^2)^{-1/2}$ (where $\beta_h c$ is the head’s velocity), exceeds the inverse beaming angle $1/\theta$. If it did, then the jet head would be causally disconnected from its edges and would behave like a spherical blastwave (Blandford & McKee 1976). In this case essentially no material would escape sideways to form the cocoon. If instead $\Gamma_h < 1/\theta$ then there is ample opportunity for shocked jet and envelope material to flow sideways and inflate the cocoon, so a successful GRB requires

$$\Gamma_h < 1/\theta \quad (\text{stellar envelope}). \quad (1)$$

Observers of GRB afterglows often identify an achromatic break in the light curve with the deceleration of the swept up shell from $\Gamma_h > 1/\theta$ to $\Gamma_h < 1/\theta$ (Rhoads 1999). In order for this to be possible, the head must have satisfied

$$\Gamma_h > 1/\theta \quad (\text{circumstellar medium}) \quad (2)$$

while it was still being driven forward by the jet (prior to its deceleration). Condition (2) only applies to GRBs whose afterglows exhibit such a break in their afterglows.

The expansion velocity of the jet head is given to a very good approximation by the balance of jet and ambient ram pressures (momentum fluxes) in the frame of the jet head. This approximation is most accurate when ambient material is cast aside into the cocoon, as is the case if equation (1) is satisfied. Ram pressure balance means

$$\rho_j h_j (\Gamma\beta)_{jh}^2 c^2 + p_j = \rho_a h_a (\Gamma\beta)_h^2 c^2 + p_a \quad (3)$$

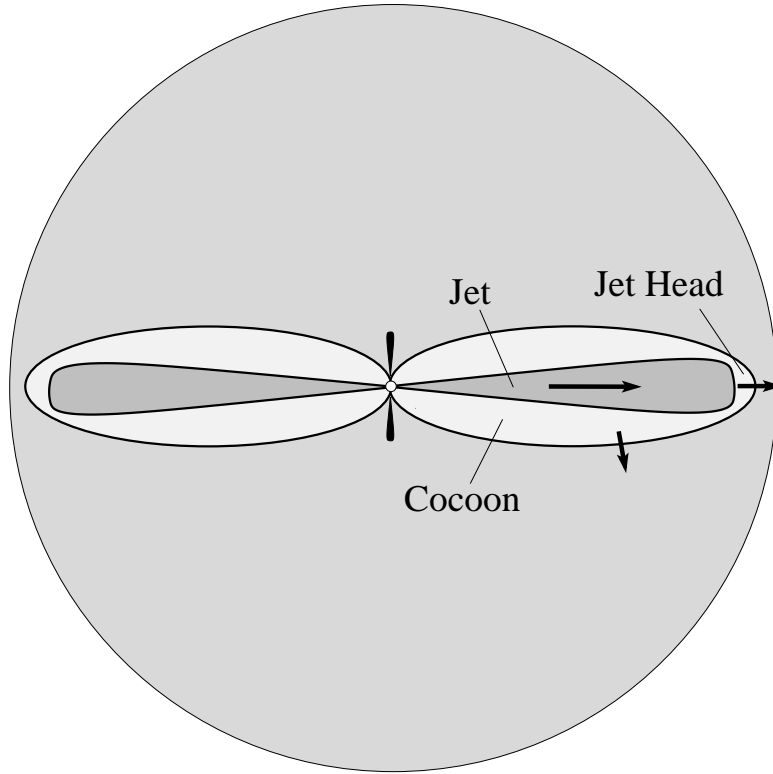


Figure 2. Schematic of a jet traversing a stellar envelope. The two collide at the jet head, from which material flows sideways into the cocoon.

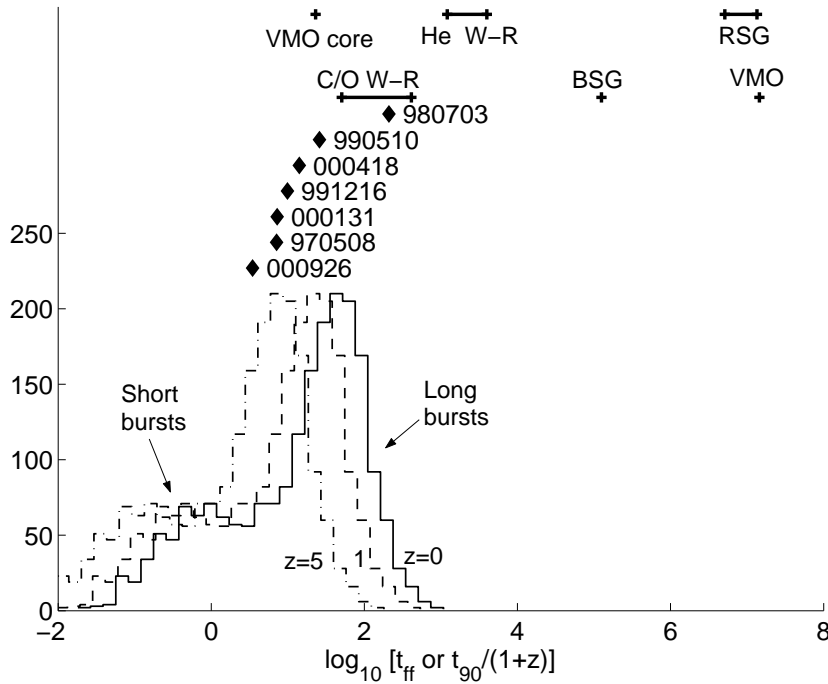


Figure 3. GRB durations compared to stellar dynamical times. The histogram of observed burst durations ($t_{90}/(1+z)$), for redshifts $z = 0$, $z = 1$ and $z = 5$ from the current BATSE catalog (<http://cossc.gsfc.nasa.gov/batse/>) is plotted to show the timescales for long and short bursts. Notable bursts with afterglow observations are plotted as diamonds and labeled. Also plotted are the typical free-fall times for carbon-oxygen (“WR: C/O”) and helium (“WR: He”) progenitors evolved from Wolf-Rayets, blue and red supergiants (“BSG” and “RSG,” respectively), the primordial $300 M_{\odot}$ progenitor (“VMO”) calculated by Fryer et al. (2001), and the $100 M_{\odot}$ core of a VMO with no envelope. For GRBs arising from SNe, this plot shows that an uncollapsed stellar envelope remains to be traversed by the jet – except in the case of especially long GRBs coming from compact carbon-oxygen stars or VMO cores.

where $(\Gamma\beta)_{jh}$ is the relative four-velocity between the jet and its head, $(\Gamma\beta)_h$ is the four-velocity of the head into the ambient medium, ρ , p , and $h \equiv (e + p)/(\rho c^2)$ are density, pressure, and enthalpy (e is total comoving energy density), and the subscripts j and a refer to jet and ambient material. As $p_a \ll \rho_a c^2$ in a stellar envelope $h_a = 1$ to a good approximation and p_a can be ignored on the right-hand side. To leading order in Γ_j^{-1} , p_j can be ignored on the left. For a stationary ambient medium, these approximations give

$$\beta_h = \frac{\beta_j}{1 + \tilde{L}^{-1/2}} \quad (4)$$

(Marti et al. 1994) where

$$\tilde{L} \equiv \frac{\rho_j h_j \Gamma_j^2}{\rho_a} = \frac{L_{\text{iso}}/c^3}{dM/dr}. \quad (5)$$

The second equality, which holds to leading order in Γ_j^{-1} , is derived by noting that the kinetic plus internal energy density of the jet, evaluated in the lab frame, is $\Gamma_j^2 h_j \rho_j - \Gamma_j \rho_j - p_j$; its isotropic luminosity L_{iso} is this quantity times $4\pi r^2 \beta_j$; and the mass per unit length of the ambient medium is $dM/dr \equiv 4\pi r^2 \rho_a$. Here r is the radius and the true jet luminosity is $L = (\theta^2/4)L_{\text{iso}}$.

The relation between Γ_h and Γ_j implied by equation (4) takes simple limits in two regimes. If $\tilde{L} \gg \Gamma_j^4$, then the reverse shock into the jet is nonrelativistic (Sari & Piran 1995) and $\Gamma_j - \Gamma_h \ll \Gamma_j$. This case is physically unattainable within a star and is achieved outside only if the ambient density is extremely low. In the opposite limit of a relativistic reverse shock,

$$\tilde{L}^{1/2} = \frac{1}{\beta_h} - 1 = \begin{cases} 2\Gamma_h^2, & \Gamma_j^4 \gg \tilde{L} \gg 1; \\ \beta_h, & \tilde{L} \ll 1 \end{cases} \quad (6)$$

(see also Mészáros & Waxman 2001). Therefore, \tilde{L} is useful in determining the observer's time $t_{\text{obs}}/(1+z) = t - r/c$ for the jet head to expand to radius r if viewed at redshift z . Since $dt = dr/(\beta c)$,

$$\frac{dt_{\text{obs}}}{1+z} = \frac{dr}{\tilde{L}^{1/2} c} \quad (7)$$

for both non-relativistic and relativistic jet heads, so long as $\tilde{L} \ll \Gamma_j^4$. In presupernova envelopes and stellar winds dM/dr is relatively constant, and since L_{iso} is likely to vary slowly \tilde{L} can be approximated with its average value. More generally, one might know how L_{iso} varies as a function of t (which is also $t_{\text{obs}}/(1+z)$ at the origin, $r = 0$). If one also knows $M(r)$ (e.g. from a model of the star and its collapse), then equation (7) integrates to

$$\int^{t_{\text{obs}}} L_{\text{iso}}(t_{\text{obs}})^{1/2} \frac{dt'}{1+z} = \int^r \left(c \frac{dM}{dr} \right)^{1/2} dr', \quad (8)$$

giving $t_{\text{obs}}(r)$ implicitly.

2.3 Cocoon Structure

The jet cocoon is the region containing spent jet material and shocked ambient material. Its extent is equal to that of the jet, but its width is determined either by pressure balance with the surrounding gas, if there is time for this to be achieved, or else by the expansion of a lateral shock into the envelope. The latter case holds so long as it predicts a cocoon

pressure p_c in excess of the hydrostatic pressure or collapse ram pressure p_a in its environment. Let us first consider the case of an adiabatic cocoon whose pressure exceeds that of its surroundings, and check this assumption in §6.1. Let us also restrict attention to the case where the head velocity is subrelativistic ($\tilde{L} < 1$, eq. [6]), in which case the cocoon pressure p_c is roughly constant away from the jet head.

The cocoon created by a jet of constant opening angle expands self-similarly so long as its width R_c expands in proportion to its extent r , and so long as no other size scales affect its structure. Under these conditions, numerical simulations can determine cocoon structures exactly. However, analytical estimates (e.g., Begelman & Cioffi 1989), while not as accurate, elucidate how cocoon properties scale with \tilde{L} and θ .

The cocoon expands nonrelativistically in a direction normal to its surface at the velocity β_c given by

$$\rho_a c^2 \beta_c^2 = p_c. \quad (9)$$

If ρ_a is evaluated at the point where the cocoon is widest, the normal direction is sideways and thus $\beta_c \simeq R_c/(ct)$. The pressure p_c is related to the energy E_{in} deposited in the cocoon and the cocoon volume V_c through $p_c \simeq E_{\text{in}}/(3\rho_a V_c)$ (an overestimate, as part of E_{in} is kinetic). If a cocoon of length r and width R_c is idealized as a cone, $V_c \simeq (\pi/3)R_c^2 r$ and $\rho_a \simeq \rho_a(r)$ in equation (9). But, since $\dot{r} = \beta_h c$ and $\dot{R}_c \simeq \beta_c c$, $V_c \simeq (\pi/3)r^3(\beta_c/\beta_h)^2$.

Now, E_{in} is the energy emitted in time to catch up with the jet head at radius r . (After breakout, E_{in} is available to drive an observable outflow and possibly a precursor: see Ramirez-Ruiz, Celotti, & Rees (2002) and §5.) As long as $\tilde{L} \ll \Gamma_j^4$ the flight time of the jet can be neglected compared to $t_{\text{obs}}(r)/(1+z)$, so $E_{\text{in}}(r)$ is essentially all of the energy emitted up to then:

$$\begin{aligned} E_{\text{in}}(r) &= \int_0^{t_{\text{obs}}(r)/(1+z)} L dt \\ &\simeq \left[\frac{\theta^4}{16} L_{\text{iso}} r M(r) c \right]^{1/2} \end{aligned} \quad (10)$$

using equation (7). Along with the expressions for p_c , V_c and β_c , this implies

$$\beta_c \simeq \tilde{L}^{3/8} \theta^{1/2}. \quad (11)$$

This implies that the cocoon is nonrelativistic (and slower than the jet head) so long as the jet head is also nonrelativistic, for $\tilde{L} < 1$ in this case (eq. [6]), and $\theta < 1$ for a collimated jet.

2.3.1 Cocoons vs. Jet-Driven Explosions

Equation (11) assumes that the length of the cocoon is set by the advance of the jet head; this requires $\beta_c < \beta_h$. If this condition is violated, the cocoon expands around the jet and develops into a roughly spherical blastwave (see also Begelman & Cioffi 1989). For a nonrelativistic jet head, equations (6) and (11) indicate that $\beta_c < \beta_h$ so long as $\tilde{L} \gtrsim \theta^4$. For a more precise criterion, consider the velocity β_{bw} of a spherical blastwave powered by two jets:

$$\beta_{\text{bw}} = 0.90 \left[\frac{2E_{\text{in}}(t = r/\beta_{\text{bw}})}{M(r)c^2} \right]^{1/2} = 0.74\theta^{2/3}\tilde{L}^{1/3}, \quad (12)$$

where the coefficient is given by the PGA/ \bar{K} approximation of Ostriker & McKee (1988), for a wind bubble with a ratio of specific heats $\hat{\gamma} = 4/3$ in a medium with $\rho_a \propto r^{-2}$. The head outruns this blastwave ($\beta_h > \beta_{bw}$) if $\tilde{L} > (\theta/90^\circ)^4$, i.e.,

$$\frac{L_{\text{iso}}r}{c} > \left(\frac{\theta}{90^\circ}\right)^4 M(r)c^2. \quad (13)$$

This condition can only be violated if $\tilde{L} < (\theta/90^\circ)^4 \ll 1$, so that only jets driving nonrelativistic heads can violate it. I assumed a nonrelativistic head in deriving equation (13); however there is nothing to suggest that relativistic jet heads can be swallowed by their cocoons.

A successful GRB requires that stellar envelope material be cleared from the path of the jet so it can sustain $\Gamma_j \gtrsim 10^2$ at $r \sim 1$ AU where internal shocks are thought to form. A jet-cocoon structure is required for this: a spherical blastwave would not accomplish it. For this reason GRBs must satisfy $(\theta/90^\circ)^4 < \tilde{L} < \theta^{-4}$ within the stellar envelope (eqs. [1], [6], and [13]) so that a cocoon forms but does not overcome the jet. Of these limits on \tilde{L} , only the lower need be considered because $\tilde{L} \ll \theta^{-4}$ for any reasonable combination of opening angle and stellar model.

One can use equation (13) in equation (10) to eliminate either $L_{\text{iso}}r/c$, which gives a lower limit on $E_{\text{in}}(r)$, or to eliminate $\theta^4 M(r)c^2$, which gives an upper limit on $E_{\text{in}}(r)$. In terms of the total energy per lobe $E_{\text{in}}(R)$ deposited in the stellar envelope, the formation of a cocoon rather than a spherical blastwave implies

$$0.10 \theta^4 M_{\text{env}} c^2 < E_{\text{in}}(R) < 0.61 L_{\text{iso}} R/c. \quad (14)$$

A spherical blastwave is not sensitive to the site of energy injection, whether at a jet head or near the collapsing core, and for this reason the upper bound applies to energy from *any* source that is entrained in the stellar envelope before the jet breaks out of the star. Note that the lower bound implies that $E_{\text{in}}(R)$ must be at least a fraction $(\theta/37^\circ)^2$ of the rest energy of the envelope in the jet's path, $(\theta^2/4)M_{\text{env}}c^2$.

2.4 Timing Constraint

One further and very important constraint derives from the durations of GRBs. In the internal-shock model, fluctuating gamma-ray emission reflects variability in the central engine and persists only while this engine is running (Sari & Piran 1995). Define $t_{\gamma,\text{obs}}$ as the observed duration of a GRB, including any precursor but excluding its afterglow. In the collapsar model, this must be preceded by the cocoon phase during which the jet crosses the stellar envelope. The central engine must therefore be active for at least $t_{\gamma,\text{obs}} + t_{\text{obs}}(R)$ in the observer's frame. It is unlikely – though not impossible – for $t_{\gamma,\text{obs}}$ to be much shorter than $t_{\text{obs}}(R)$, for this would require the central engine to shut off just as its effects become observable. So

$$\frac{t_{\text{obs}}(R)}{1+z} \lesssim t_{\gamma}; \quad \varepsilon_{\gamma} E_{\text{in}}(R) \lesssim E_{\gamma}, \quad (15)$$

where ε_{γ} is the efficiency with which the jet's kinetic luminosity is converted into gamma rays in the observed band. The second inequality derives from the first as long as the jet's luminosity is relatively constant.

2.5 Jet variability

I have assumed a constant luminosity jet up to this point, but GRBs are often observed to fluctuate significantly in intensity on very short timescales. How should the above results be adjusted for jet variability? First, note that the process producing gamma rays (e.g., internal shocks) is likely to accentuate the intrinsic variability of the source. Second, the observed propagation speed of the jet head, dr/dt_{obs} , is equal to $c\tilde{L}^{1/2}$ (eq. [7]). A fluctuating jet thus progresses more slowly than a steady jet of the same mean luminosity. If one uses the average value of \tilde{L} to constrain a star's mass and radius by requiring that $t_{\text{obs}}(R)$ is not long compared to the observed burst (eqs. [15] above and [18] below), then this constraint is only tightened if one accounts for variability. Similarly, a variable jet deposits more energy per radius than a steady jet of the same mean luminosity; this only tightens the constraints derived by requiring a jet-cocoon structure (eq. [13]).

3 CONSTRAINTS ON STELLAR HOSTS

To apply the above constraints to stellar progenitors for GRBs, observed quantities must be related to the parameters of equations (13), (14), and (15). This is possible for cases where, in addition to $t_{\gamma,\text{obs}}$, the redshift z and jet opening angle θ have been derived from afterglow observations. To construct \tilde{L} one requires the isotropic (equivalent) kinetic luminosity L_{iso} and the mass per unit radius dM/dr in the environment.

I adopt for GRBs' energy, luminosity, and duration the following definitions: $L_{\gamma,\text{iso}} \equiv E_{\gamma,\text{iso}}(1+z)/t_{\gamma,\text{obs}}$; and $\{E_{\gamma}, L_{\gamma}\} \equiv \{E_{\gamma,\text{iso}}, L_{\gamma,\text{iso}}\} \times \theta^2/4$. Here the isotropic gamma ray energy is $E_{\gamma,\text{iso}}$, and ε_{γ} is the average efficiency factor relating the gamma-ray energy to the total (kinetic, Poynting, and photon) luminosity of the jet. The net energy E and luminosity L represent only the approaching jet, which presumably has a counterjet.

A key assumption employed throughout this section is that the γ -ray half opening angle θ is equal to the jet's half opening angle while it crosses the outer stellar envelope. This is essentially the same as the assumption that the jet is ballistic (rather than hot and pressure-confined) at that point; this assumption is revisited in §6. I assume the value of θ derived from afterglow observations (Rhoads 1999) can be used to characterize the jet as it crosses the outer stellar envelope and emerges from the star. The above definitions identify $L_{\gamma,\text{iso}}$ as the mean value (energy E_{γ} in source-frame duration $t_{\gamma,\text{obs}}/(1+z)$). This is somewhat arbitrary, since GRBs are highly variable; see §2.5 for justification.

For numerical evaluations I use either $L_{\gamma,\text{iso},51} \equiv L_{\gamma,\text{iso}}/10^{51}$ erg/s, or $E_{\gamma,50.5} \equiv E_{\gamma}/10^{50.5}$ erg. The former is a characteristic value for GRBs and can be observed without determining θ . The latter is motivated by Frail et al. (2001)'s result that $E_{\gamma} = 10^{50.5 \pm 0.5}$ erg for ten GRBs whose θ could be determined.

In a stellar envelope the radial average value of dM/dr is M_{env}/R , the ratio of envelope mass to stellar radius. Indeed, many presupernova envelopes have density profiles close to $\rho_a \propto r^{-2}$ (Chevalier 1989), for which dM/dr is constant at

its average value. The average value of \tilde{L} is

$$\tilde{L} = 1.30 \times 10^{-3} \frac{L_{\gamma\text{iso},51}}{\varepsilon_\gamma} \frac{R}{R_\odot} \frac{M_\odot}{M_{\text{env}}} \quad (\text{envelope}). \quad (16)$$

In order for the jet head to be relativistic ($\tilde{L} > 1$), the star must have a mass per length much lower than M_\odot/R_\odot , or the gamma-ray efficiency ε_γ must be small.

3.1 Constraints from Burst Duration and Cocoon Formation

Under the assumption of a ballistic jet, the observed time of jet breakout is

$$t_{\text{obs}}(R) = 64.4(1+z) \left(\frac{\varepsilon_\gamma}{L_{\gamma\text{iso},51}} \frac{R}{R_\odot} \frac{M_{\text{env}}}{M_\odot} \right)^{1/2} \text{ s}. \quad (17)$$

This, along with the constraint $t_{\text{obs}}(R) \lesssim t_{\gamma,\text{obs}}$ (eq. [15]) illustrates that typical long-duration GRBs are most easily produced in compact stars (MacFadyen et al. 2001). This constraint is best expressed

$$\varepsilon_\gamma \frac{M_{\text{env}}}{M_\odot} \frac{R}{R_\odot} \lesssim L_{\gamma\text{iso},51} \left[\frac{t_{\gamma,\text{obs}}/(1+z)}{64.4 \text{ s}} \right]^2; \quad (18)$$

the left-hand side pertains to a hypothetical stellar model and to the efficiency of gamma radiation and is constrained by observables on the right. Note that the combination $L_{\gamma\text{iso},51} [t_{\gamma,\text{obs}}/(1+z)]^2$ is related to an observed burst's fluence and duration through its comoving distance (i.e., physical distance at redshift zero), rather than its luminosity distance. Note also that the above constraint is independent of θ .

In figure 4 I illustrate the derivation of $L_{\text{iso}} t_{\text{obs}}^2 / (1+z)^2$ and constraint (18) from the observed fluence and duration and an observed or estimated redshift (for $\Omega_m = 0.3$, $\Lambda = 0.7$, $H_0 = 65 \text{ km s}^{-1} \text{ Mpc}^{-1}$). Bursts with well-observed redshifts are plotted as solid diamonds; those for which Fenimore & Ramirez-Ruiz (2000) have estimated redshifts from a luminosity-variability correlation are plotted as open circles. A progenitor model passes the timing constraint if it lies to the left of its burst. Most of the bursts plotted are consistent with $\varepsilon_\gamma M_{\text{env}} R \lesssim 10 M_\odot R_\odot$; for none of them does this limit exceed $90 M_\odot R_\odot$. This constraint is nearly independent of redshift and derives primarily from the distribution of (fluence $\cdot t_{\text{obs}}$) among GRBs. VMO cores and Wolf-Rayet stars are compatible with many bursts. Blue supergiants are compatible only with the very brightest and longest. Red supergiants and VMOs that retain their envelopes are ruled out, as are optically-thick shrouds of expanding ejecta which might persist in the ‘‘supernova’’ or stellar-merger models of central engines.

Equation (13) gives a complimentary constraint on the basis that a jet-cocoon structure exists:

$$\varepsilon_\gamma \frac{M_{\text{env}}}{M_\odot} \frac{R_\odot}{R} < L_{\gamma\text{iso},51} \left(\frac{17.0^\circ}{\theta} \right)^4. \quad (19)$$

This constraint is derived from observations of bursts in figure 5. Similar to figure 4, filled diamonds here represent bursts for which afterglow observations have allowed an estimate of θ in addition to L_{iso} (as reported by Frail et al. 2001, and references therein); open circles represent redshifts estimated by Fenimore & Ramirez-Ruiz (2000). For these I

have estimated θ by requiring that $E_\gamma = 10^{50.5}$ erg as suggested by Frail et al. (2001). These points fall in a narrow band on the plot because $L_{\gamma\text{iso}}/\theta^4 = (1+z)E_\gamma/(\theta^4 t_{\text{obs}})$. With E_γ held fixed, the dispersion in this quantity is dominated by θ^{-4} (2 dex rms, for the points plotted) rather than $(1+z)/t_{\text{obs}}$ (0.5 dex rms).

4 CONSTRAINTS ON STELLAR WINDS

GRBs from supernovae are likely to occur within a dense stellar wind, an environment that potentially affects both the GRB itself and its afterglow (Kumar & Panaitescu 2000; Ramirez-Ruiz, Dray, Madau, & Tout 2001).

The internal-shock model for GRB emission posits that significant variability on a time scale δt ($\equiv \delta t_{\text{obs}}/(1+z)$) arises from the collision of shells within the jet at radii of about

$$r_{\text{IS}} \equiv 2\Gamma_j^2 c \delta t, \quad (20)$$

as discussed by Rees & Meszaros (1994). Sari & Piran (1995) argue that an external shock with the ambient medium – to which the afterglow is attributed – cannot create a fluctuating gamma ray burst. For internal shocks to occur, the external shock (jet head) must move beyond r_{IS} on a timescale not long compared to the duration of the burst: $\Delta t_{\text{obs}}(r_{\text{IS}}) \lesssim t_{\gamma,\text{obs}}$.

Sari & Piran (1995) define $N_p \equiv t_{\gamma,\text{obs}}/\delta t_{\text{obs}}$ as the number of pulses that fit within the burst duration given a characteristic separation δt_{obs} . With equations (6), (20), and this definition, the criterion $\Delta t_{\text{obs}}(r_{\text{IS}}) \lesssim t_{\gamma,\text{obs}}$ becomes

$$\Gamma_h^2 \gtrsim \frac{\Gamma_j^2}{N_p}, \quad (21)$$

or

$$\tilde{L} \gtrsim \frac{4\Gamma_j^4}{N_p^2} = 4 \times 10^4 \left(\frac{\Gamma_j}{100} \right)^4 \left(\frac{100}{N_p} \right)^2. \quad (22)$$

Sari & Piran argue that $N_p \sim 100$ is typical, although a wide variety of time scales is observed within bursts (Lee et al. 2000).

For a wind dM/dr is the ratio of mass loss rate to wind velocity, \dot{M}_w/v_w , so

$$\tilde{L} = \frac{5.89 \times 10^6}{\varepsilon_\gamma} \frac{L_{\gamma\text{iso},51} v_{w,8}}{\dot{M}_{w,-5}} \quad (\text{wind}) \quad (23)$$

where $v_{w,8} \equiv v_w/(10^8 \text{ cm s}^{-1})$ and $\dot{M}_{w,-5} \equiv \dot{M}_w/(10^{-5} M_\odot \text{ yr}^{-1})$ are normalized to characteristic values for Wolf-Rayet stars (Nugis & Lamers 2000), although the presupernova mass loss rates of such stars is not well known (Langer 1991). Expressing condition (22) in terms of Γ_j ,

$$\Gamma_j < 350 \left(\frac{N_p}{100} \right)^{1/2} \left(\frac{L_{\gamma\text{iso},51} v_{w,8}}{\varepsilon_\gamma \dot{M}_{w,-5}} \right)^{1/4}. \quad (24)$$

The analogous criterion for a uniform ambient medium was presented by Piran (1999). This upper limit on Γ_j must exceed the lower limit required for the escape of the observed gamma rays, described most recently by Lithwick & Sari (2001). These authors inferred $\Gamma_j > 340$ for five of the ten ordinary bursts in their Table 2; equation (24) suggests that

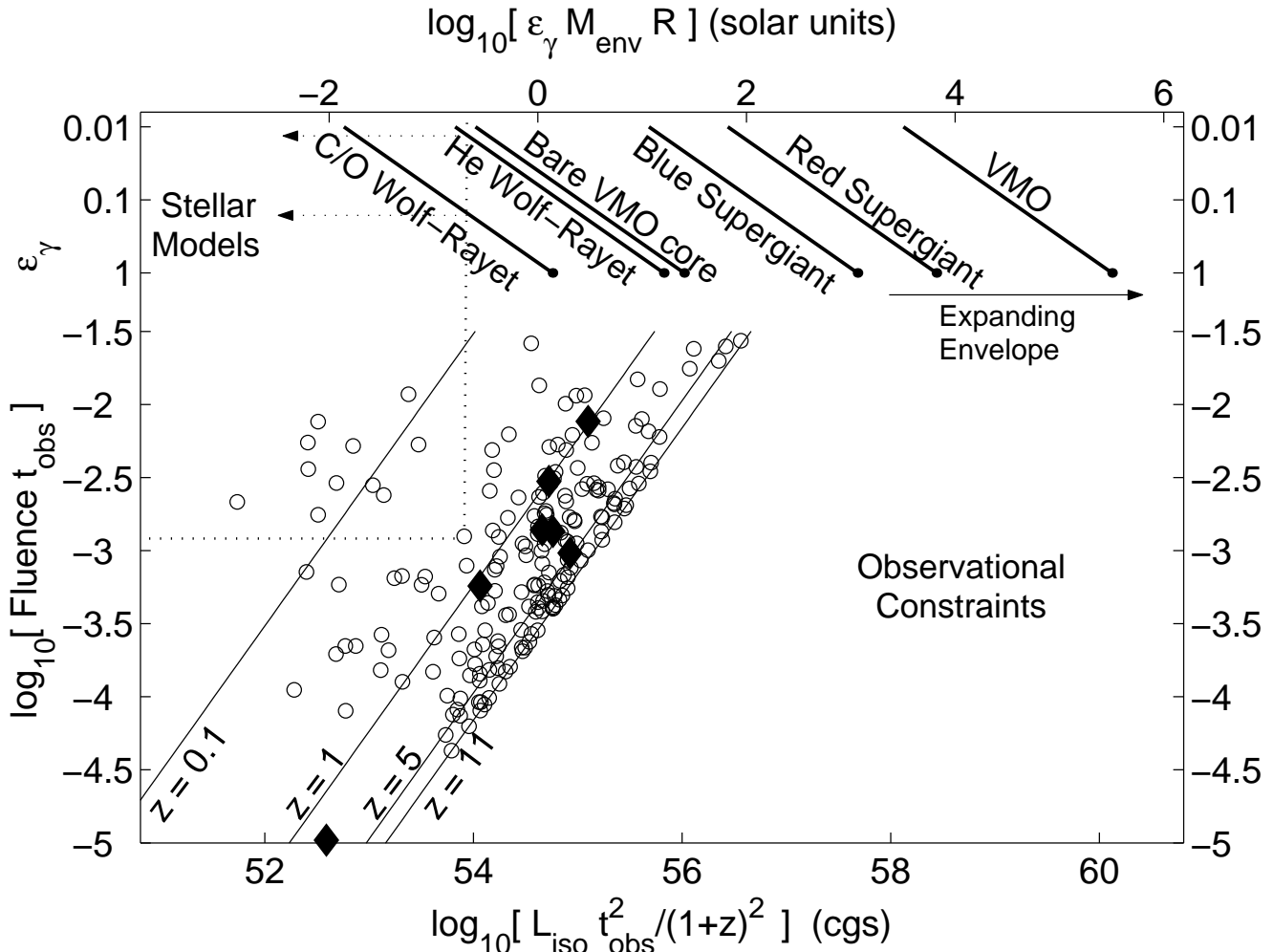


Figure 4. The product of a GRB’s fluence and duration constrains the product of mass and radius in any stellar envelope through which the GRB jet (if moving ballistically: see §6) could have emerged rapidly compared to the period of emission. The observed quantity fluence $\cdot t_{\text{obs}}$ and the redshift imply the quantity $L_{\text{iso}} t_{\text{obs}}^2 / (1+z)^2$ intrinsic to the burst. By eq. (18), this places an upper limit on the model parameter $\varepsilon_{\gamma} M_{\text{env}} R$, where ε_{γ} is the efficiency of gamma-ray production; so, a model should lie to the left of its burst on the plot. This limit insensitive to GRB redshift when $z > 1$. In this plot *solid diamonds* are the bursts plotted in figure 3, with redshifts and fluences derived from Frail et al. (2001) and references therein; *circles* are 220 bursts for which Fenimore & Ramirez-Ruiz (2000) estimate redshifts using a luminosity-variability correlation (these authors did not allow $z > 11$). The burst illustrated with *dotted lines* is compatible with a carbon-oxygen post-Wolf-Rayet progenitor if $\varepsilon_{\gamma} \lesssim 15\%$, or with a helium-bearing post-Wolf-Rayet star or the $100 M_{\odot}$ bare core of a very massive object (VMO) if $\varepsilon_{\gamma} \lesssim 3\%$. (For other VMO core masses, use $M_{\text{env}} R \propto M^{3/2}$ at O ignition.) It is not compatible with blue or red supergiant progenitors (BSGs or RSGs), VMOs that have not lost their radiative envelopes, or the expanding envelope of the “supranova” progenitor of Vietri & Stella (1999) (not shown), which moves to the right on this plot. Similar conclusions can be drawn for almost all of the bursts plotted. Lines of constant z are shown for $\Lambda = 0.7$, $\Omega_m = 0.3$, $H_0 = 65 \text{ km s}^{-1} \text{ Mpc}^{-1}$.

these could not have occurred in a stellar wind representative of Wolf-Rayet stars – unless, for instance, $N_p \gg 100$ (which does not appear to characterize the bursts in their Table 2).

However, condition (24) might be circumvented by the efficient sweeping-forward of the ambient medium by run-away pair production, as discussed by Madau & Thompson (2000), Thompson & Madau (2000) and Beloborodov (2002). If the relativistic flow has generated a fraction of the observed photons at a radius smaller than r_{IS} , then these can clear optically-thin ambient gas from the region.

A spreading break (albeit one difficult to detect:

Kumar & Panaitescu 2000) will occur in the afterglow if equation (2) is satisfied. The remaining isotropic kinetic luminosity after the gamma-rays have been emitted is $(1 - \varepsilon_{\gamma}) L_{\gamma \text{iso}} / \varepsilon_{\gamma}$. Along with (23), this becomes

$$\theta > 1.64^{\circ} \left[\frac{\varepsilon_{\gamma} \dot{M}_{w,-5}}{(1 - \varepsilon_{\gamma}) L_{\gamma \text{iso},51} v_{w,8}} \right]^{1/4}. \quad (25)$$

This criterion could only be violated by the narrowest of GRB jets in especially dense stellar winds.

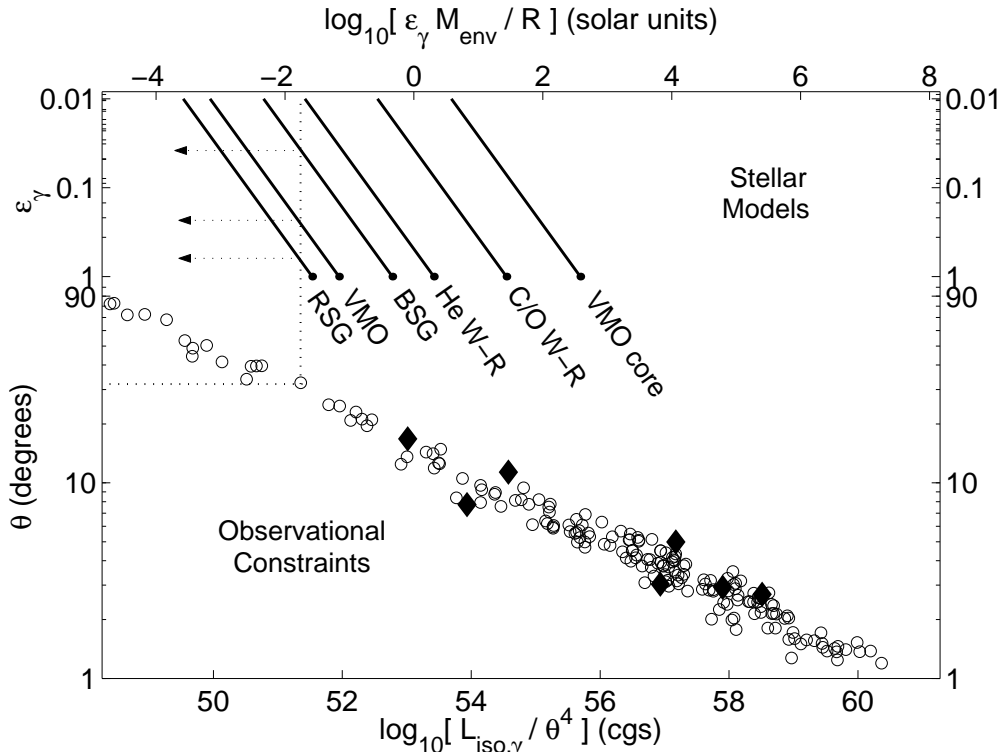


Figure 5. The opening angle and isotropic luminosity of a GRB – in the combination $L_{\text{iso}}\theta^{-4}$, eq. (19) – constrain the ratio of mass and radius in any envelope through which the GRB’s jet can travel without being engulfed within its own bubble. (The jet is assumed to be moving ballistically; see §6.) As in figure 4, a viable model should lie to the left of its GRB on the plot. Here, the constraint is most sensitive to θ . *Filled diamonds* represent bursts with θ inferred from afterglow observations (Frail et al. 2001, and references therein). *Open circles* are the bursts for which Fenimore & Ramirez-Ruiz (2000) estimate redshifts; for these θ is estimated under the assumption of a common energy $E_{\gamma} = 10^{50.5}$ erg (causing θ to correlate tightly with $L_{\gamma\text{iso}}$). Most bursts are compatible with all stellar progenitors by this criterion; however, those with large θ are not. Diffuse stars most easily pass this test. VMO cores fail first, when $\theta \simeq 10^{\circ}$ (plotted is a $100 M_{\odot}$ core; $M_{\text{env}}/R \propto M^{1/2}$ at O ignition). The burst illustrated by *dotted lines* is compatible with RSGs, VMOs that retain their envelopes, BSGs, and helium post-Wolf-Rayet stars for values of ε_{γ} less than 90%, 50%, 3%, and 1%, respectively. The supernova model travels to the left on this plot as it expands, and easily passes this constraint.

5 BREAKOUT AND BLOWOUT: OBSERVATIONAL CONSEQUENCES

The energy deposited by the jet as it crosses a surrounding stellar envelope (E_{in} in §2) is available to power (conceivably) observable phenomena distinct from the GRB and its afterglow. These include transients associated with the emergence of the jet head from the stellar surface (*breakout*), and the escape of hot cocoon material along the path of the jet (*blowout*). Note that a type Ic light curve is not a product of jet energy, as SN Ic are powered by radioactive nickel, which is not produced at the jet head.

The energy E_{in} is typically less than the total GRB jet energy (for successful GRBs) according to condition (15). Nevertheless the effects of deposited energy may be of observational interest if they cover a wider opening angle, dominate a different observed band, are emitted with higher efficiency, or occur where the jet stalls before breakout.

5.1 Shock Acceleration and Breakout

In ordinary supernovae the fastest ejecta are produced at the surface of the star. There, the rapid decrease in stellar density leads to a whip-like acceleration of the shock

front followed by additional postshock acceleration (Sakurai 1960). Sufficiently energetic explosions can produce relativistic ejecta this way, so long as the stellar progenitor is sufficiently compact (Matzner & McKee 1999). The impact of these ejecta with a circumstellar wind may produce a transient of hard photons; this is a plausible explanation for the association between supernova 1998bw and GRB 980425 (Matzner & McKee 1999; Tan et al. 2001; Matzner, Tan, & McKee 2001).¹

MacFadyen & Woosley (1999), MacFadyen et al. (2001), and Zhang, Woosley, & MacFadyen (2003) have suggested that shock breakout might lead to the X-ray precursors seen in some bursts (Laros et al. 1984; Murakami et al. 1991; in ’t Zand et al. 1999). MacFadyen & Woosley and MacFadyen et al. concentrate on the prompt flash from the shock-heated stellar photosphere; however, the fast ejecta have a greater store of kinetic energy to be tapped. Lyutikov & Usov (2000) discuss several cases of precursor

¹ SN 2003dh, which appeared in the afterglow of GRB 030329, appears similar to SN 1998bw; however, the Tan et al. model cannot explain a two-peak GRB of $\sim 10^{51.5}$ erg emerging from a SN of comparable energy.

activity in gamma rays, including one burst for which iron-line emission has been suggested (GRB 991216: Vietri et al. 2001). If precursors are due to shock breakout then their energy is a small fraction of $E_{\text{in}}(R)$ and is therefore limited by conditions (14) and (15); however it may yet be observable. In 't Zand et al. (1999) argue that the X-ray precursor of GRB 980519 resembles its X-ray afterglow to the extent that the afterglow effectively preceded the GRB; as argued by Paczynski (1998), this is consistent with the emission from material with $\gamma < \Gamma_j$ ejected prior to the GRB emission. It is therefore worthwhile to estimate the distribution of ejecta kinetic energies from shock breakout in a jetlike explosion.

To do this one must identify at what point the jet head makes a transition from the state of ram pressure balance described in §2.2 to the state of whip-like shock acceleration discussed by Tan et al. (2001). The jet head obeys ram pressure balance only if shocked ambient material exits the jet head more rapidly than the head accelerates. While this holds, the forward ambient shock cannot travel far ahead of the jet reverse shock. At some point near the surface, however, ambient material cannot exit the jet head prior to breakout. The forward shock will then accelerate away down the density gradient, and the flow becomes progressively more normal to the surface (Tan et al. 2001).

If β_{\perp} is a typical value for the perpendicular component of velocity in the jet head, and $x \equiv (R-r)/R$ is the fractional depth within the stellar envelope, then material is trapped within the head if $(\theta R)/\beta_{\perp} > (xR)/\beta_h$, i.e., if the time to exit the head exceeds the time to reach the surface. A reasonable guess for β_{\perp} is that shocked ambient gas exits the jet head at the postshock sound speed, in the frame of the head. For a nonrelativistic head, then, $\beta_{\perp} \simeq (8/49)^{1/2}\beta_h$. In the relativistic case, the transverse velocity saturates at $\sim c/\sqrt{3}$ in the head's frame; in the star's frame, $\beta_{\perp} \simeq 1/(3^{1/2}\Gamma_h)$ (Rhoads 1999). So the transition occurs when

$$x = \theta \times \begin{cases} (49/8)^{1/2}\phi_{nr}, & \tilde{L}(x) \ll 1; \\ 3^{1/2}\Gamma_h\phi_r, & \tilde{L}(x) \gg 1 \end{cases} \quad (26)$$

where $(\phi_{nr}, \phi_r) \sim 1$ are uncertain parameters. In the relativistic case, x is determined implicitly once $\Gamma_h(x)$ is known. For this, apply equation (4) to the outer density distribution of the stellar progenitor

$$\rho_a = \rho_h \left(\frac{x}{1-x} \right)^n, \quad (27)$$

where n is the effective polytropic index and the coefficient ρ_h is an extrapolation to $r = R/2$. In a radiative outer layer ρ_h can be derived from the mass, radius, and luminosity of the progenitor star (Kippenhahn & Weigert 1994; Tan et al. (2001) present formulae (their equations [25], [45], and [48]) for ρ_h in Kramers or Thomson atmospheres.

Once x and $\beta_h(x)$ or $\Gamma_h(x)$ have been identified, the production of fast ejecta follows from Tan et al. (2001)'s theory (their eq. [54]) if one matches the shock four-velocity $\gamma_s\beta_s$ with the head four-velocity $\Gamma_h\beta_h$ at the depth x . With equations (4) and (26) setting a reference depth, external mass, and shock velocity, their theory predicts an isotropic-equivalent ejecta kinetic energy

$$E_{k,\text{iso}}(> \Gamma_f) = \frac{(\phi_{nr}\theta)^{-1.65n\gamma_p}\Gamma_f^{-(1.58\gamma_p-1)}}{(n+2.70)\exp(1.98+7.03/n-1.52n)}$$

$$\times \left(\frac{L_{\text{iso}}}{R^2\rho_h c^3} \right)^{2.68\gamma_p-1} L_{\text{iso}} \frac{R}{c}, \quad (28)$$

when the transition occurs in the nonrelativistic regime, and

$$E_{k,\text{iso}}(> \Gamma_f) = \frac{(\phi_r\theta)^{-\frac{0.317\gamma_p}{4\gamma_p-3}}\Gamma_f^{-(1.58\gamma_p-1)}}{(n+2.70)\exp\left[\frac{(n+3.26)(n+6.69)}{1.22n(n+4)}\right]} \times \left(\frac{L_{\text{iso}}}{R^2\rho_h c^3} \right)^{\frac{4.32\gamma_p-3}{n(4\gamma_p-3)}} L_{\text{iso}} \frac{R}{c}, \quad (29)$$

when the head is relativistic at the transition. Here, $\gamma_p \equiv 1 + 1/n$ is the envelope's polytropic exponent. These equations have been simplified by the restriction $\Gamma_f \gg 1$.

In general, the appropriate value of $E_{k,\text{iso}}(> \Gamma_f)$ is the minimum of the values given by equations (28) and (29). Note that $E_{k,\text{iso}}(> \Gamma_f)$ is an isotropic equivalent; the *total* kinetic energy per lobe in ejecta above Γ_f is smaller by $\theta^2/4$. If one varies θ holding the other quantities fixed, this total energy above Γ_f is maximized when the two expressions are equal, whereas the isotropic value continues to rise slowly as θ is decreased in the relativistic regime. In the relativistic regime, the above formulae only apply to $\Gamma_f > \Gamma_h(x)^{2.73}$ – i.e., only to those ejecta involved in quasi-spherical shock acceleration.

The uncertainty of $(\phi_{nr}, \phi_r) \times \theta$ leads to a much greater uncertainty in $E_{k,\text{iso}}(> \Gamma_f)$ for the nonrelativistic than for the relativistic case: for instance, when $n = 3$, $E_{k,\text{iso}}(> \Gamma_f)$ varies as $(\phi_{nr}\theta)^{-6.7}$ in the nonrelativistic and as $(\phi_r\theta)^{-0.19}$ in the relativistic regime. Physically, this difference arises because ram pressure and shock acceleration give very different velocity laws in the nonrelativistic regime ($\beta_h \propto \rho_a^{-1/2}$ and $\beta_s \propto \rho_a^{-0.187}$, respectively) whereas they give very similar velocity laws in the relativistic regime ($\Gamma_h \propto \rho_a^{-1/4}$ and $\Gamma_s \propto \rho_a^{-0.232}$, respectively). Another uncertainty concerns whether the head velocity should be matched to the shock or postshock velocity; the latter choice increases the ejecta energies by only 6 – 7% for both relativistic and nonrelativistic transitions.

5.1.1 An Example: the SN 1998bw Progenitor

To illustrate these estimates of jet-driven shock breakout, let us consider the progenitor model for SN 1998bw adopted by Woosley et al. (1999) and studied by Tan et al. (2001). The parameters n , R , and ρ_h can be derived from Tan et al.'s tables 2 and 3. Adopting their fit for the outermost regions (whose rest energy is $< 1.7 \times 10^{50}$ erg), $n = 4$, $\rho_h = 335 \text{ g cm}^{-3}$, and $R = 1.4 \times 10^{10} \text{ cm}$. The isotropic kinetic energy in breakout ejecta is therefore:

$$E_{k,\text{iso}}(> \Gamma_f) \simeq \min \left[1.9 \left(\frac{L_{\gamma\text{iso},51}}{\varepsilon_{\gamma}} \right)^{1.3} \left(\frac{\phi_r\theta}{2.5^{\circ}} \right)^{-0.20}, \right. \\ \left. 2.1 \left(\frac{L_{\gamma\text{iso},51}}{\varepsilon_{\gamma}} \right)^{3.3} \left(\frac{\phi_{nr}\theta}{2.5^{\circ}} \right)^{-8.4} \right] \times 10^{48} \Gamma_f^{-0.975} \text{ erg}. \quad (30)$$

If this formula were to give a result $> 2 \times 10^{50}$ erg, a different envelope fit would be appropriate; however, the qualitative result would be unchanged.

Even in isotropic equivalent, the energy predicted by equation (30) is small compared to a cosmological GRB. It is

comparable in magnitude to the values derived by Tan et al. for the spherical explosion of SN 1998bw. While sufficient to produce GRB 980425 at a redshift of 0.0085, it would not contribute to the appearance of a GRB at $z \gtrsim 1$.

It should not be surprising that the energy of motion in shock breakout is intrinsically much smaller than that available in the jet, as the accelerating shock is powered by the jet for a brief period (a small range of radii) prior to breakout. Breakout does produce a spray of ejecta with a variety of Lorentz factors, which may produce weak transients if observed off the jet axis.

5.2 Cocoon Blowout

The cocoon inflated by a jet prior to breakout is filled with hot gas that is free to expand away from the star after breakout, constituting a “dirty” fireball (Paczynski 1998) which may be visible either through its thermal emission, through its circumstellar interaction, or through line absorption and fluorescence. The cocoon energy E_{in} (eq. 10) comprises

$$4.4 \times 10^{49} \left[\frac{L_{\gamma\text{iso},51}}{\epsilon_\gamma} \left(\frac{M_{\text{env}}}{M_\odot} \right) \left(\frac{R}{R_\odot} \right) \right]^{1/2} \left(\frac{\theta}{3^\circ} \right)^2 \text{ erg.} \quad (31)$$

Ramirez-Ruiz, Celotti, & Rees (2002) have considered observable implications of cocoon blowout under the hypothesis that no mixing occurs between shocked jet and shocked envelope material, so that the cocoon fireball can accelerate to Lorentz factors comparable to Γ_j . A likely alternative is some mixing between jet and envelope, especially near the jet head where shear is strong. Suppose the shocked jet mixes with the envelope material within an angle $\phi_{\text{mix}}\theta$ of the jet axis before entering the cocoon: $\phi_{\text{mix}} \simeq 1$ for mixing near the jet head only. The energy per mass of the hot cocoon material is then $(2/\phi_{\text{mix}})\tilde{L}^{1/2}c^2$, corresponding to a subrelativistic outflow velocity

$$\begin{aligned} v_{\text{out}} &= \frac{\sqrt{2}}{\phi_{\text{mix}}} \tilde{L}^{1/4} c \\ &= \frac{0.27}{\phi_{\text{mix}}} \left[\left(\frac{R}{R_\odot} \right) \left(\frac{M_\odot}{M_{\text{env}}} \right) \left(\frac{L_{\gamma\text{iso},51}}{\epsilon_\gamma} \right) \right]^{1/4} c \end{aligned} \quad (32)$$

where I assume $\tilde{L} \ll 1$ as is appropriate for the compact progenitors favored in §3. If blowout occurs into an angle θ_{out} , then the expanding cocoon material becomes optically thin ($\tau < 1$) along its axis after roughly

$$\begin{aligned} 14 & \left[\left(\frac{\epsilon_\gamma}{L_{\gamma\text{iso},51}} \right) \left(\frac{R_\odot}{R} \right) \right]^{1/4} \left(\frac{M_{\text{env}}}{M_\odot} \right)^{3/4} \\ & \times \left(\frac{\kappa}{0.4 \text{ cm}^2 \text{ g}^{-1}} \right)^{1/2} \frac{\phi_{\text{mix}}(\theta/3^\circ)}{\theta_{\text{out}}} \text{ hours.} \end{aligned} \quad (33)$$

Before this occurs, however, photons will diffuse sideways out of the blowout cloud when the lateral optical depth $\tau_{\text{lat}} \simeq \theta_{\text{out}}\tau$ and lateral velocity v_{lat} satisfy $\tau_{\text{lat}} \simeq c/(3v_{\text{lat}})$. This occurs at ~ 13 hours for the fiducial parameters listed above (independently of θ_{out}); the amount of internal energy persisting in the ejecta is quite small by that point, indicating that a thermal pulse will not be observed unless the fireball is enriched with short-lived isotopes. The modest cocoon energy is available for circumstellar interaction but may be masked by the GRB afterglow. The cocoon blowout

does, however, represent a screen between the jet-afterglow shock on the outside and the expanding SN ejecta and central engine on the inside.

6 PRESSURE CONFINEMENT

Two assumptions made in sections 2 and 3 remain to be checked, both concerning the effects of an external pressure on the cocoon or on the jet. §6.1 addresses the assumption that the cocoon drives a strong shock into the stellar envelope. §6.2 concerns the possibility that the jet is self-confined by its own cocoon pressure, then spreads sideways outside the star before producing gamma rays.

6.1 Ambient pressure confinement

If the ambient pressure is greater than the pressure within the cocoon, then the assumption of a strong shock in equation (9) is incorrect and the cocoon does not inflate as described in §2.3. The cocoon is overpressured relative to the envelope by $(\beta_c c)^2/c_s^2$, where c_s is the envelope’s isothermal sound speed:

$$c_s(r)^2 = \frac{p_a(r)}{\rho_a(r)} \equiv \alpha(r) \frac{GM(r)}{3r}. \quad (34)$$

With $\alpha(r)$ so defined, the virial theorem stipulates $\langle \alpha \rangle = 1$ when the mean is weighted by binding energy and $\langle 1/\alpha \rangle = 1$ when weighted by thermal energy within the star. In general, $\alpha(r) \sim 1$ wherever the scale height is of order the radius. (In a polytrope of index n , α is related to Chandrasekhar 1939’s variable v by $3/\alpha = (n+1)v$.) Using equations (11) and (34), $p_c > p$ when

$$\begin{aligned} L &\gtrsim \frac{3\theta_j^{2/3}}{4\alpha} \left(\frac{c_s}{c} \right)^{14/3} \frac{c^5}{G} \\ &= \frac{\theta_j^{2/3} \alpha^{4/3}}{17.3} \left[\frac{GM(r)}{rc^2} \right]^{7/3} \frac{c^5}{G}. \end{aligned} \quad (35)$$

This constraint is expressed in terms of the total jet luminosity L ; I shall evaluate it at the fiducial collapse temperature $T_9 \simeq 3.2$ (O ignition; Bond et al. 1984). The appropriate value of θ_j , though different from θ_γ , cannot exceed unity.

In ordinary core-collapse supernovae (below the pair instability limit) the core is degenerate but the envelope above the collapsing core is not; also, gas pressure dominates over radiation pressure. At the oxygen ignition temperature, condition (35) becomes

$$L \gtrsim 3.2 \times 10^{50} \alpha^{-1} \theta_j^{2/3} \left[\left(\frac{T_9}{3.2} \right) \left(\frac{2}{\mu} \right) \right]^{7/3} \text{ erg s}^{-1} \quad (36)$$

where μ is the mean mass per particle in a.m.u.

In contrast to ordinary supernova cores, VMO cores are dominated by radiation and are approximately $n = 3$ polytropes in structure (Bond et al. 1984). They obey $R_{\text{core}} = 0.26[M_{\text{core}}/(100 M_\odot)]^{1/2}(3.2/T_9) R_\odot$; hence $p_c > p_a$ when

$$\begin{aligned} L &\gtrsim 1.3 \times 10^{51} \alpha^{4/3} \theta_j^{2/3} \left(\frac{T_9}{3.2} \right)^{7/3} \\ &\times \left(\frac{M_{\text{core}}}{100 M_\odot} \right)^{7/6} \text{ erg s}^{-1}. \end{aligned} \quad (37)$$

The critical luminosities in equations (36) and (37) should be compared to the value $L \simeq 3 \times 10^{50} (10\%/\epsilon_\gamma) (10 \text{ s}/t_\gamma) \text{ erg s}^{-1}$ implied by Frail et al. (2001)'s standard value $E_\gamma = 10^{50.5} \text{ erg}$. In both ordinary supernovae and collapsing VMOs, the jet cocoon could possibly be pressure-confined in the collapsing region ($T_9 \gtrsim 3$), but not in the hydrostatic region where $T_9 \lesssim 1$.

6.2 Self-confinement by cocoon pressure

The constraints on stellar envelopes derived above assume that observational determinations of the intensity (L_{iso}) and opening angle of gamma-ray emission can be applied to the earlier phase in which the GRB crossed the stellar envelope. This requires that the jet is dynamically cold in the stellar interior, so that it does not widen once outside the star. It is important to consider the alternative: that the jet may contain internal energy sufficient to spread in angle after breakout. In this case the emission angle θ_γ will exceed the jet angles θ_j attained within the stellar envelope. The jet would then be more intense within the star than outside, vitiating (or at least relaxing) the constraints on stellar envelopes derived in §§2 and 3.

For the flow to expand after breakout it must possess relativistic internal energy, $h_j \rho_j \simeq 4p_j$, and it must be slow enough to spread, $\Gamma_j < 1/\theta_j$. (Note that cold jets will be heated and decelerate locally to $\Gamma_j < 1/\theta_j$, if they are crossed by an stationary oblique shock.) In this case the final opening angle will be set by the relativistic beaming of the jet at breakout: $\theta_\gamma \simeq 1/\Gamma_j$; a suggestion made by R. Blandford. In general,

$$\begin{aligned} \theta_\gamma &\simeq \frac{1}{\Gamma_j(r_{\text{conf}})} + \theta_j(r_{\text{conf}}) \\ &\simeq \max[1/\Gamma_j(r_{\text{conf}}), \theta_j(r_{\text{conf}})] \end{aligned} \quad (38)$$

where the two possibilities refer to hot, confined jets (with the confining pressure is released at r_{conf}) and cold, ballistic jets, respectively.² One must have $r_{\text{conf}} \simeq R$ for pressure confinement to be significant; if $r_{\text{conf}} \ll R$, the ballistic-jet constraints of the previous section would still hold for the outer envelope. For confined jets, $\Gamma_j(R)$ is determined by an observational determination of the final opening angle. At the same time, when $h_j \rho_j \simeq 4p_j$, and so long as Γ_j is still significantly above unity, the jet luminosity is

$$L = 4\pi R_j^2 \Gamma_j^2 p_j c \quad (\text{hot jet})$$

(see the discussion after equation [5]), where $R_j \equiv \theta_j r$ is the jet radius. If evaluated at r_{conf} , Γ_j may be replaced with $1/\theta_\gamma$.

What determines p_j ? The confining pressure is clearly time-dependent in this scenario, which complicates matters, but one can set $p_j \simeq p_c$ at r_{conf} . The cocoon pressure is $\rho_a (\beta_c c)^2$ where β_c is given by equation (11):

$$L^3 \rho_a = \pi^3 c^9 R_j^2 r^4 p_c^4,$$

² Zhang, Woosley, & MacFadyen (2003) suggest eq. (38) does not describe their numerical results; however, it is not clear what r_{conf} or $\Gamma_j(r_{\text{conf}})$ is applicable to the wide-angle ejecta they see. Although the choice of a single r_{conf} is perhaps oversimplified, it remains a useful parameterization.

the primary assumption being that the jet head expands nonrelativistically ($\dot{L} < 1$). Setting $p_j = p_c$ and using $\Gamma_j = 1/\theta_\gamma$,

$$2^4 (cR_j^2)^3 \pi \rho_a = \theta_\gamma^8 r^4 L \quad (\text{cocoon - confined, hot jet}) \quad (39)$$

which provides a means to evaluate pressure confinement if one has a constraint on R_j .

6.2.1 Adiabatic jets

One such constraint arises if the jet expands adiabatically from its launching region, since this provides a formula for $R_j(p_j)$. For the steady flow of a relativistically hot gas ($p_j \gg \rho_j c^2$) at relativistic speeds ($\beta_j \simeq 1$) through a channel, the simultaneous conservation of luminosity $L = (4\Gamma_j^2 p_j) \pi R_j^2 c$ and mass flux $\dot{M} = \Gamma_j \rho_j \pi R_j^2 c$, along with the relation $p_j \propto \rho_j^{4/3}$, imply

$$\Gamma_j(r) = \frac{R_j}{r_0} \quad \text{and} \quad p_j(r) = \frac{L}{4\pi r_0^2 c} \Gamma_j^{-4} \quad (\text{adiabatic jet}) \quad (40)$$

where r_0 is the radius from which the flow accelerates through $\Gamma_j = 1$ and should reflect the dimensions of the central engine, tens or hundreds of kilometers. In equation (39), this implies

$$\begin{aligned} \theta_\gamma &= 1.6 \left(\frac{c^3 r_0^6 \rho_a}{L r^4} \right)^{1/14} \\ &= 0.93^\circ \left(\frac{r_0}{10 \text{ km}} \right)^{3/7} \left(\frac{\rho_a}{1 \text{ g cm}^{-3}} \right)^{1/14} \\ &\quad \times \left(\frac{10^{52} \text{ erg s}^{-1}}{L} \right)^{1/14} \left(\frac{R_\odot}{r} \right)^{2/7}. \end{aligned} \quad (41)$$

The γ -ray opening angle produced by pressure confinement of an adiabatic jet is thus lower than any of the derived opening angles, the discrepancy being much greater in terms of pressure (since $p_j/p_c \propto \theta_\gamma^{-3.5}$ at fixed r_0).

A jet expanding adiabatically from $r_0 \sim 10 \text{ km}$ can therefore be confined in the core of the star, but would become cold and ballistic in the outer envelope. We found in §6 that the ambient core pressure may be high enough crush the cocoon, suggesting that the jet can also be confined by ambient pressure in this region. This scenario was described by Mészáros & Rees (2001); as they note, it holds only in the stellar core and fails (producing a ballistic jet of fixed $\theta_j = \theta_\gamma$) in the envelope. However, we must question whether r_0 might also change.

6.2.2 Nonadiabatic jets: crossing shocks and mixing

The above argument shows that a jet expanding from a launching region r_0 of order 10 km will no longer be pressure-confined in the outer stellar envelope. But, what if the propagation is not adiabatic? This can result from shocks that cross the jet, or from mixing between the jet and its environment (cocoon or stellar envelope). Heuristically one expects the jet's memory of r_0 to be erased in either process; a larger effective r_0 would ameliorate the discrepancy highlighted in §6.2, perhaps making pressure confinement more realistic.

First, consider a stationary oblique shock that crosses the jet. The postshock jet pressure (p_{j2}) is brought into

equilibrium with p_c , the external pressure that launches the shock. The shock front must be causal with respect to the postshock flow, i.e., sound travels across the (post-shock) jet faster than the shock itself does. If the postshock Lorentz factor is Γ_{j2} , sound fronts can propagate at an angle $1/(\sqrt{3}\Gamma_j)$ to the jet axis. This must exceed the angle θ_{cs} of the crossing shock relative to the jet axis (although usually not by much: Whitham 1974). In order for the shock to cross the jet, one must have $\theta_{cs} > \theta_j$; so, $\Gamma_{j2} \lesssim 1/(\sqrt{3}\theta_{cs}) < \theta^{-1}$. The jet therefore makes a transition to a hot, pressure-confined state at its current radius; the new effective value of r_0 for the postshock jet is $R_j/\Gamma_{j2} \gtrsim \sqrt{3}\theta_{cs}R_j$.

One can, in fact, estimate Γ_{j2} and the shock obliquity θ_{cs} from the expression $L_j = 4\pi R_j^2 \Gamma_{j2}^2 p_{j2} c$ (valid for hot jets), from the condition $\Gamma_{j2} \lesssim 1/(\sqrt{3}\theta_{cs})$, and from the requirement that $p_{j2} \simeq p_c$. If $p_c = \beta_c^2 \rho_a c^2$ is estimated via equation (11), one finds

$$\frac{\theta_{cs}}{\theta_j} \simeq 3.5 \left[\frac{M_{\text{env}} R_\odot}{M_\odot R} \frac{10^{52} \text{erg/s}}{L_j} \left(\frac{3^\circ}{\theta_j} \right)^2 \right]^{1/8}, \quad (42)$$

which can be read as an estimate of the number of crossing shocks along the jet axis. Note that eq. (38) predicts $\theta_\gamma \simeq \theta_{cs}$, roughly speaking, if the jet is effectively released after one of its crossing shocks. These results appear broadly compatible with the work of Zhang, Woosley, & MacFadyen (2003), and indicate the potential importance of this route to pressure confinement.

Second, consider the mixing of ambient material into the jet during a pressure-confined phase. Nonadiabatic mixing can be described by imagining relativistically hot jet material flowing through a uniform channel of fixed cross-sectional area A_j . At some initial time the channel is allowed to mix with some area dA_j of ambient material (density ρ_c , pressure p_c) at rest. Assuming perfect mixing and nonrelativistic surroundings ($p_c \ll \rho_c c^2$), the change in jet parameters p_j , ρ_j , and Γ_j are determined by the conservation of energy, momentum, and rest mass through the mixing event. That is,

$$d \left(\left\{ \begin{array}{c} \Gamma_j^2 h_j \rho_j - p_j \\ \Gamma_j^2 \beta_j h_j \rho_j \\ \Gamma_j \rho_j \end{array} \right\} A_j \right) = \left\{ \begin{array}{c} \rho_c c^2 \\ 0 \\ \rho_c \end{array} \right\} dA_j. \quad (43)$$

Algebra then yields differential equations for p_j , ρ_j , and Γ_j as functions of A .

A couple interesting conclusions can be drawn from this exercise. First, the heuristic argument that r_0 would be forgotten is correct: the effective value of $r_0 \equiv R_j/\Gamma_j$ increases monotonically in non-adiabatic jet expansion, because R_j increases whereas Γ_j decreases (or if $\rho_c = p_c = 0$, stays constant). This in turn implies that pressure confinement is extended somewhat by mixing.

Secondly, mixing forces the nondimensional jet parameters to trace a characteristic trajectory that whose implications would be observable. Recall that the final opening angle θ_γ is the inverse of Γ_j if the jet is confined. Also, final Lorentz factor Γ_f is equal to the ratio of the jet's luminosity to its mass flux,

$$\eta_j \equiv \frac{L_j}{\dot{M}_j c^2} = \left(\frac{4p_j}{\rho_j c^2} + 1 \right) \Gamma_j.$$

In terms of these dimensionless parameters, equation (43)

can be restated

$$\frac{d\Gamma_j}{d \ln M_j} = -\Gamma_j^2 \frac{(4\Gamma_j^2 - 1)(\Gamma_j^2 - 1)}{\eta_j(2\Gamma_j^2 + 1) + \Gamma_j^3 - \Gamma_j}; \quad (44)$$

$$\frac{d\eta_j}{d \ln M_j} = -\eta_j \frac{\eta_j + 2\Gamma_j^2(\eta_j - 2) + \Gamma_j^3}{\eta_j(2\Gamma_j^2 + 1) + \Gamma_j^3 - \Gamma_j}, \quad (45)$$

where $d \ln M_j = \rho_c dA/(\Gamma_j \rho_j A)$ represents the fractional mass per unit length mixed in. The ratio of these equations (in which the denominators cancel) describes set mixing trajectories for $\eta_j(\Gamma_j)$, as shown in fig. 6. There exists an attractor solution, which is $\eta = 4\Gamma_j^2$ (i.e., $p_j = \Gamma_j \rho_j c^2$) when $\Gamma_j \gg 1$ and approaches $(\eta_j, \Gamma_j) \rightarrow (1, 1)$. Mixing trajectories rapidly join onto it by decreasing either Γ_j or η_j as mass is mixed in.

As shown in figure 6, mixing trajectories do cross through reasonable values of Γ_f and θ_γ . Does this mean that these jet parameters arise from mixing? This seems plausible if there ever exists phase of pressure-confined evolution in the stellar core or mantle. If $2\Gamma_j < \eta_j^{1/2}$, adiabatic expansion and mixing both act to bring $2\Gamma_j \rightarrow \eta_j^{1/2}$. If $2\Gamma_j > \eta_j^{1/2}$, the adiabatic tendency for Γ_j to increase is counterbalanced by the nonadiabatic decrease in Γ_j . This makes the mixing attractor solution a probable one for the end state of jets that are pressure-confined at some stage. (A more detailed analysis would require a dynamical analysis of jet expansion.)

If so, then the attractor solution would imprint the correlation

$$\theta_\gamma \simeq 11^\circ \left(\frac{100}{\Gamma_f} \right)^{1/2} \quad (\text{mixing attractor}) \quad (46)$$

which may have observational implications in that $L_{\gamma_{\text{iso}}} \propto \Gamma_f$ for a fixed L_j/ϵ_γ . Such a trend has been implicated in the correlations between spectral lag and luminosity, variability and luminosity, and afterglow break time and luminosity among GRBs (e.g., Ramirez-Ruiz & Lloyd-Ronning 2002; Salmonson & Galama 2002). The mixing attractor provides a motivation for a rather tight correlation among bursts with similar jet luminosities.

6.2.3 Confined jets: timing properties

The variability-luminosity correlation would be affected also by the filtering of jet variations by pressure gradients, which occurs only when the jet is pressure-confined. Now, the internal dynamical time of a relativistic jet is $\sim R_j/c$, or $\Gamma_j R_j/c$ in the lab frame. If a strobe approached the observer at Γ_j , pulsating once per dynamical time, the observed period would be foreshortened to

$$\delta t_{\text{obs}} \simeq \frac{R_j}{\Gamma_j c} = \frac{r_0}{c}. \quad (47)$$

The same result can be derived by considering a standing-wave pattern of wavelength R_j in the jet's frame, or R_j/Γ_j in the lab frame, that is swept past a fixed pressure-release radius r_{conf} and leads to jet pulsations as the peaks and troughs pass by. As we saw above, crossing shocks and mixing increase the effective value of r_0 and thus increase the characteristic variability timescale. Shocks and mixing also decrease $L_{\gamma_{\text{iso}}}$ by decreasing Γ_j and thereby increasing θ_γ ; this implies a correlation between jet variability and γ -ray brightness.

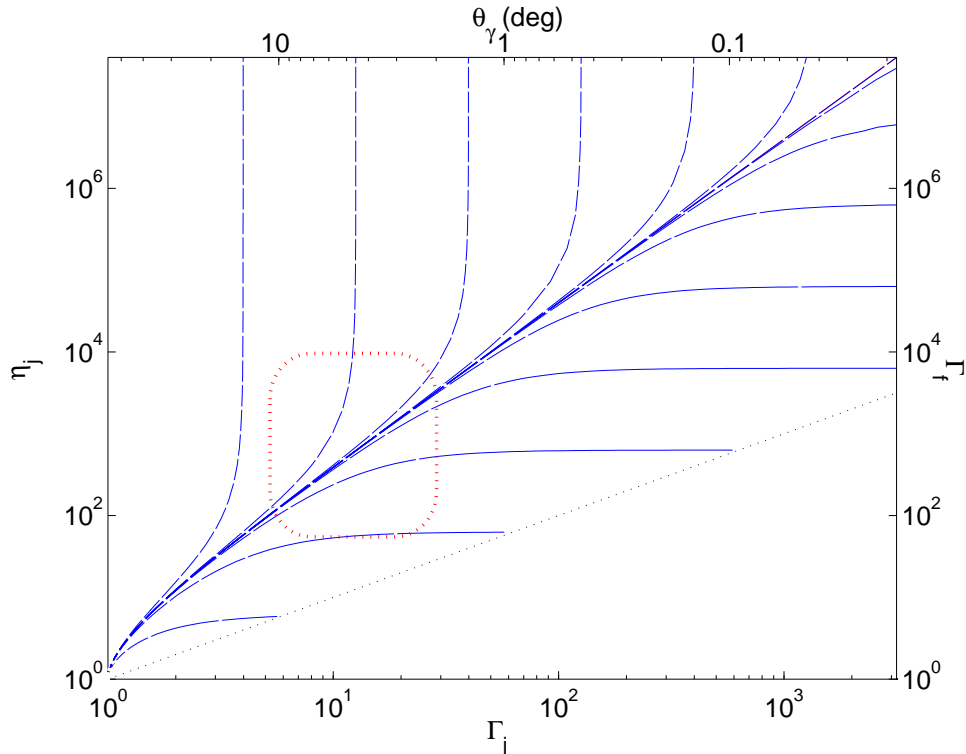


Figure 6. Evolution of pressure-confined jets due to mixing with their surroundings (eqs. [44] and [45]). The ratio η_j of luminosity to mass flux is plotted versus jet Lorentz factor; these set the final Lorentz factor Γ_f and opening angle θ_γ . Breaks in the trajectories are spaced by a doubling of jet mass per unit length. Mixing causes jets to move down and to the left along the plotted trajectories toward $\eta_j = \Gamma_j = 1$. In contrast, adiabatic evolution causes jets to move horizontally rightward to higher Γ_j (smaller θ_γ) at fixed η_j and Γ_f . No solutions exist below the dotted line ($\eta_j = \Gamma_j$), where pressure is negative. Accepted ranges of θ_γ and Γ_f are estimated by the dotted rectangle. Inside this region, mixing correlates observables: higher Γ_f corresponds to lower θ_γ .

6.3 Pressure Confinement and Envelope Constraints

What should we make of the possibility that pressure-confined jets will evade the constraints on stellar envelopes derived in §§2 and 3 for ballistic jets? Equation (41) shows that jet confinement works if

$$r_0 = 500 \left(\frac{\theta_\gamma}{5^\circ} \right)^{7/3} \left(\frac{r_{\text{conf}}}{R_\odot} \right)^{2/3} \left(\frac{1 \text{ g cm}^{-3}}{\rho_a} \right)^{1/6} L_{52}^{1/6} \text{ km},$$

a value that does not appear to violate timing constraints (eq. [47]). This indicates pressure-confined jets are plausible if shocks or jet mixing increase r_0 sufficiently.

Why would a jet change from pressure-confined to ballistic? This could occur in a couple ways. First, the jet could accelerate in such a way that sound no longer crosses it despite it being hot, i.e., $\Gamma_j(r) > 1/\theta_j(r)$ for some range of r . However this appears to require the ambient density to drop to a near vacuum, implying it would not occur spontaneously within a star. Alternatively, the jet could become internally nonrelativistic ($p_j \lesssim \rho_j c^2$). As we have seen, adiabatic evolution works in this direction whereas crossing shocks and non-adiabatic mixing oppose it. The transition would then depend on the specifics of jet propagation and mixing. Finally, the jet could be confined by internal magnetic stresses, a possibility highlighted by the γ -ray polarization discovered by Coburn & Boggs (2003), but beyond the scope of this paper.

Jet pressure confinement would naturally lead to time-dependent jet properties, since the confining pressure evolves during the cocoon phase and after breakout. Crossing shocks and mixing with ambient material are also unlikely to be steady processes. One would expect evolution during GRBs as a result; however, no trends are discernible except for changes in pulse asymmetry (Lee et al. 2000).

Apart from this contraindication, it is difficult to judge whether pressure confinement persists across entire stellar radii. If so, then the constraints on stellar envelopes in §§2 and 3 are relaxed. Numerical simulations can potentially solve detailed questions such as this one. However, caution should be used in interpreting them, because of the many decades separating the launching radius from the stellar radius.

7 CONCLUSIONS

This paper constrains possible stellar progenitors for GRBs by requiring that jets of GRB-like luminosities and durations can clear a path for themselves in the star's envelope prior to producing gamma rays. Of all the possible progenitors, only the compact carbon-oxygen post-Wolf-Rayet stars (SN Ic progenitors) and the bare cores of very massive objects can plausibly collapse in the durations of long GRBs at low redshift (§2.1, figures 1 and 3). In more extended stars, the outer stellar envelope remains to impede the progress of

the jet, and it is likely to violate observational constraint. Therefore, I conclude that GRBs with SN progenitors come primarily from type Ic or VMO-core events. Type Ib is not thoroughly ruled out by this work, but type II (supergiant stars) are.

The most stringent constraint on a stellar envelope arises from the requirement that the jet can traverse it in an observed time not much longer than the duration of the GRB. Under the assumption of a ballistic rather than a pressure-confined jet, this constraint is independent of the inferred opening angle of the burst, and (given an observed fluence and duration) depends on its inferred comoving distance rather than its luminosity distance. This makes it insensitive to an uncertainty in redshift. Given the luminosities and durations of GRBs (regardless of their redshift; fig. 4), only post-Wolf-Rayet stars and VMO cores are compact enough to satisfy this criterion. The variability-luminosity correlation discussed by Fenimore & Ramirez-Ruiz (2000) and Reichart et al. (2001) allows this constraint to be applied to a large number of bursts in the BATSE catalog (figure 4). Only a few are compatible with blue supergiant progenitors; red supergiants and VMOs with envelopes are ruled out. Also ruled out is the “supranova” model of Vietri & Stella (1999) (a supernova followed by a GRB), unless the SN ejecta are optically thin by the time of the GRB, or unless the pulsar nebula is energetic enough to clear them aside.

Post-Wolf-Rayet stars have been favored among stellar GRB progenitors since the work of MacFadyen & Woosley (1999), on the basis that their compact envelopes delay the GRB jet breakout the least. The above constraint quantifies and strengthens this conclusion, and relates it to the observed properties of GRBs rather than those of a specific model for the central engine.

For ballistic jets, an additional constraint arises from the requirement that the GRB jet cocoon should not overtake its driving jet and produce a spherical explosion. This is generally not as restrictive as the constraint from burst durations discussed above, but it does become important for jets with opening angles exceeding 10° (figure 5). VMO cores, being the most compact, are the progenitors most likely to be ruled out this way if they have not collapsed prior to the GRB. The requirement of a jet-cocoon structure also gives interesting upper and lower bounds on the energy entrained in the stellar envelope during the phase of jet propagation (eq. [14]). This energy is stored in the jet cocoon and is available to drive a “dirty” fireball (Paczynski 1998) of expanding cocoon material after the jet breaks out.

The breakout phenomenon is itself a candidate for producing a transient, as may have happened in SN 1998bw to produce GRB 980425. In section 5 it is calculated how much kinetic energy is channeled into relativistic envelope ejecta during a jet’s breakout, by matching the propagation law for the jet’s terminal shock onto the relativistic shock and post-shock acceleration behavior described by Tan et al. (2001). I find the energy of this ejecta to be small compared to that of the burst. Ramirez-Ruiz, MacFadyen, & Lazzati (2002) have recently discussed how the upscattering of photons from the shocked envelope by the jet may produce a precursor of hard gamma rays; however, note that this is reduced in importance for the compact stellar progenitors favored by the timing constraints. Zhang, Woosley, & MacFadyen

(2003) have suggested breakout ejecta as the origin of short, hard bursts; however their estimate of the energy is at odds with that calculated here.

If the gamma-ray photons are not able to clear away a stellar wind in the region around the star in the manner described by Madau & Thompson (2000), Thompson & Madau (2000), and Beloborodov (2002), then the presence of this wind places an upper limit on the jet Lorentz factor. This limit arises in the internal shock model for GRB emission because the presence of the external shock limits the distance within which internal shocks can form. The equivalent limit has been presented previously for uniform ambient media Piran (1999); however, for a sufficiently dense stellar wind it can conflict with the lower limits on jet Lorentz factor (e.g., Lithwick & Sari 2001).

Figure 7 illustrates the above criteria for the specific case of GRB 000418, assuming a ballistic jet with $\epsilon_\gamma = 10\%$. Its seven-second duration is briefer even than the free-fall times of VMO cores. Because of its large opening angle (11° ; Berger et al. 2001), it would not successfully form a jet-cocoon structure in any uncollapsed portion of the VMO core. In fact, a jet of its inferred luminosity could cross nothing more extended than the most compact of Wolf-Rayet stars in the GRB duration. I conclude from this that it came either from a compact carbon-oxygen Wolf-Rayet star, or from a VMO core that managed to produce a GRB of briefer duration than its free-fall time, or that it did not have a supernova origin. These restrictions change quantitatively, but not qualitatively, if $\epsilon_\gamma \ll 10\%$.

Pressure confinement of jets provides a way for GRB hosts to evade the constraints on stellar envelopes listed above for ballistic jets. This occurs because, for a given γ -ray opening angle, confined jets are narrower and more intense than their ballistic counterparts. The computational results of Aloy et al. (2000) and Zhang, Woosley, & MacFadyen (2003) correspond to pressure-confined jets. In §6.2.1 it was shown that jets that do not mix with their environs cannot remain pressure-confined (see also Mészáros & Rees 2001). Simulations that do not resolve the jets’ launching scale may not observe this effect, however. Mixing of jet and envelope (§6.2.2) is capable of sustaining a pressure-confined state.

Intriguingly, mixing of jet and envelope imprints on the jet a tight correlation (the “mixing attractor” of eq. [46] and figure 6) between its Lorentz factor and energy per unit mass. This leads to a correlation between final opening angle and Lorentz factor, which in turn may be related to the lag-luminosity and variability-luminosity correlations observed in burst catalogs. Excessive mixing, however, has the effect of filtering rapid fluctuations from jets.

This work was stimulated by a visit to UC Santa Cruz and by interactions with Stan Woosley, Andrew MacFadyen, Alex Heger, and Weiqun Zhang while I was there. It was further motivated by conversations with and encouragement from Roger Blandford, Re’em Sari, Sterl Phinney and Josh Bloom during a visit to Caltech. It is a pleasure to thank Woosley, Blandford, and Phinney for their hospitality during those visits. I am especially grateful to Nicole Lloyd-Ronning for explaining the GRB luminosity-variability relation and suggesting clarifications. I also thank Andrei Beloborodov and Chris Thompson for discussing jet-envelope interactions and Chris Fryer for discussing progenitor scenarios. Comments from Beloborodov, Charles Dermer, Jonathan Tan,

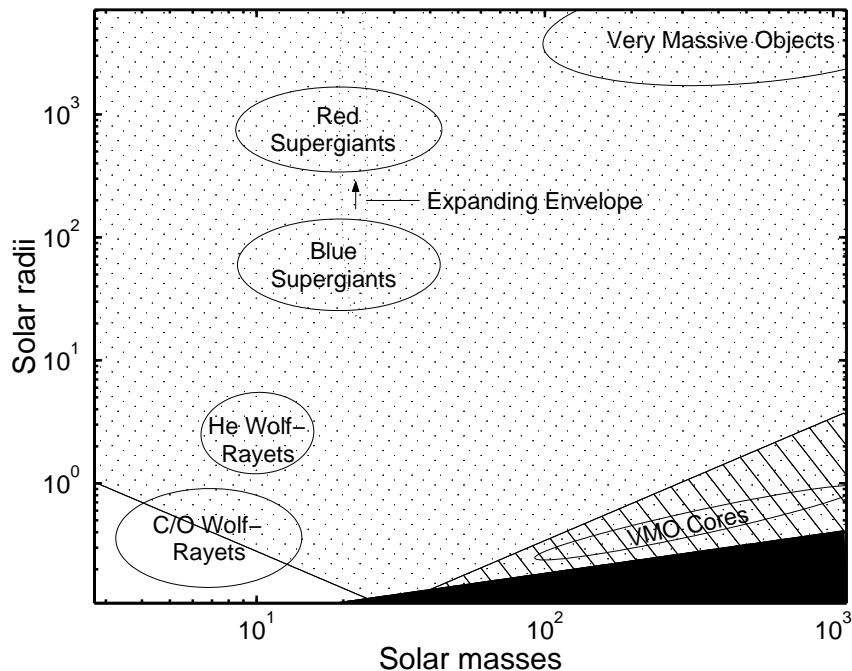


Figure 7. Constraints on possible stellar progenitors for the case of GRB 000418 (assuming a ballistic jet and $\epsilon_\gamma = 10\%$). Stars in the *black shaded region* would collapse in the seven-second intrinsic duration of the burst. Those within the *hatched region* are excluded because they are too dense for a jet-coocoon structure to exist given the luminosity of this burst, and would develop a spherical blastwave instead. Those in the *dotted region* are also excluded because the GRB jet would take much longer than the observed duration to traverse their envelopes.

Chris McKee, John Monnier, and the referee, Ralph Wijers, are also appreciated. This work was supported by NSERC and by the Canada Research Chairs program.

REFERENCES

- Aloy M. A., Müller E., Ibáñez J. M., Martí J. M., MacFadyen A., 2000, *ApJ*, 531, L119
- Baumgarte, T. W. & Shapiro, S. L. 1999, *ApJ*, 526, 941
- Böttcher M., Fryer C. L., 2001, in *Revista Mexicana de Astronomia y Astrofisica Conference Series Vol. 10, Iron lines from GRBs: Clues toward the progenitor*. pp 182–185
- Begelman M. C., Cioffi D. F., 1989, *ApJ*, 345, L21
- Beloborodov, A. M. 2002, *ApJ*, 565, 808
- Berger E., Diercks A., Frail D. A., Kulkarni S. R., Bloom J. S., Sari R., Halpern J., Mirabal N., Taylor G. B., Hurley K., Pooley G., Becker K. M., Wagner R. M., Terndrup D. M., Statler T., Wik D. R., Mazets E., Cline T., 2001, *ApJ*, 556, 556
- Björnsson, G., Hjorth, J., Jakobsson, P., Christensen, L., & Holland, S. 2001, *ApJ*, 552, L121
- Blandford R. D., McKee C. F., 1976, *Physics of Fluids*, 19, 1130
- Bloom, J. S., Kulkarni, S. R., & Djorgovski, S. G. 2002, *AJ*, 123, 1111
- Bloom, J. S. et al. 1999, *Nature*, 401, 453
- Bloom J. S., Sigurdsson S., Pols O. R., 1999, *MNRAS*, 305, 763
- Bond J. R., Arnett W. D., Carr B. J., 1984, *ApJ*, 280, 825
- Chandrasekhar S., 1939, *An introduction to the study of stellar structure*. (Chicago, Ill., University of Chicago Press)
- Chary, R., Becklin, E. E., & Armus, L. 2002, *ApJ*, 566, 229
- Chevalier R. A., 1989, *ApJ*, 346, 847
- Coburn, W. & Boggs, S. E. 2003, *Nature*, 423, 415
- Colgate, S. A. 1968, *Canadian Journal of Physics*, 46, 476
- Dermer, C. D. & Mitman, K. E. 1999, *ApJ*, 513, L5
- Djorgovski, S. G., Frail, D. A., Kulkarni, S. R., Bloom, J. S., Odewahn, S. C., & Diercks, A. 2001, *ApJ*, 562, 654
- Djorgovski, S. G. et al. 2001, *Gamma-ray Bursts in the Afterglow Era*, 218
- Esin A. A., Blandford R., 2000, *ApJ*, 534, L151
- Fenimore E. E., Ramirez-Ruiz E., 2000, *ApJ*, submitted; astro-ph/0004176
- Frail, D. A. et al. 1999, *ApJ*, 525, L81
- Frail, D. A. et al. 2002, *ApJ*, 565, 829
- Frail D. A., Kulkarni S. R., Sari R., Djorgovski S. G., Bloom J. S., Galama T. J., Reichart D. E., Berger E., Harrison F. A., Price P. A., Yost S. A., Diercks A., Goodrich R. W., Chaffee F., 2001, *ApJ*, 562, L55
- Frail D. A., Kulkarni S. R., Sari R., Taylor G. B., Shepherd D. S., Bloom J. S., Young C. H., Nicastro L., Masetti N., 2000, *ApJ*, 534, 559
- Freedman D. L., Waxman E., 2001, *ApJ*, 547, 922
- Fryer C. L., Woosley S. E., 1998, *ApJ*, 502, L9
- Fryer C. L., Woosley S. E., Heger A., 2001, *ApJ*, 550, 372
- Fryer C. L., Woosley S. E., Herant M., Davies M. B., 1999, *ApJ*, 520, 650
- Galama, T. J. et al. 1998, *Nature*, 395, 670
- Galama T. J., Wijers R. A. M. J., 2001, *ApJ*, 549, L209
- Harrison, F. A. et al. 2001, *ApJ*, 559, 123
- Hartquist T. W., Cameron A. G. W., 1977, *Ap&SS*, 48,

- 145
- Holland S., Fynbo J. P. U., Hjorth J., Gorosabel J., Pedersen H., Andersen M. I., Dar A., Thomsen B., Møller P., Björnsson G., Jaunsen A. O., Natarajan P., Tanvir N., 2001, *A&A*, 371, 52
- in 't Zand J. J. M., Heise J., van Paradijs J., Fenimore E. E., 1999, *ApJ*, 516, L57
- Iwamoto, K. et al. 1998, *Nature*, 395, 672
- Kippenhahn R., Weigert A., 1994, *Stellar Structure and Evolution. Stellar Structure and Evolution*, Springer-Verlag New York
- Kumar, P. & Panaitescu, A. 2000, *ApJ*, 541, L9
- Langer N., 1991, in "Supernovae", ed. S.E. Woosley (Springer-Verlag, New York), 1991, p. 549
- Laros J. G., Evans W. D., Fenimore E. E., Klebesadel R. W., Shulman S., Fritz G., 1984, *ApJ*, 286, 681
- Lazzati, D. et al. 2001, *A&A*, 378, 996
- Lee A., Bloom E. D., Petrosian V. ., 2000, *ApJS*, 131, 1
- Li Z., Chevalier R. A., 2001, *ApJ*, 551, 940
- Lithwick, Y. & Sari, R. 2001, *ApJ*, 555, 540
- Lyutikov M., Usov V. V., 2000, *ApJ*, 543, L129
- Mészáros P., Rees M. J., 2001, *ApJ*, 556, L37
- Mészáros P., Waxman E., 2001, *PRL*, 87, 1102
- MacFadyen A. I., Woosley S. E., 1999, *ApJ*, 524, 262
- MacFadyen A. I., Woosley S. E., Heger A., 2001, *ApJ*, 550, 410
- Madau P., Thompson C., 2000, *ApJ*, 534, 239
- Marti J. M., Mueller E., Ibanez J. M., 1994, *A&A*, 281, L9
- Matzner C. D., McKee C. F., 1999, *ApJ*, 510, 379
- Matzner C. D., McKee C. F., 2000, *ApJ*, 545, 364
- Matzner, C. D., Tan, J. C., & McKee, C. F. 2001, *AIP Conf. Proc.* 587: *Gamma 2001: Gamma-Ray Astrophysics*, 200
- Murakami T., Inoue H., Nishimura J., van Paradijs J., Fenimore E. E., 1991, *Nature*, 350, 592
- Nugis T., Lamers H. J. G. L. M., 2000, *A&A*, 360, 227
- Ostriker J. P., McKee C. F., 1988, *Rev. Mod. Phys.*, 60, 1
- Paczynski B., 1998, *ApJ*, 494, L45
- Panaitescu A., Kumar P., 2001, *ApJ*, 554, 667
- Piran T., 1999, *Physics Reports*, 314, 575
- Price, P. A. et al. 2001, *ApJ*, 549, L7
- Price, P. A. et al. 2002, *ApJ*, 572, L51
- Ramirez-Ruiz, E., Dray, L. M., Madau, P., & Tout, C. A. 2001, *MNRAS*, 327, 829
- Ramirez-Ruiz, E. & Lloyd-Ronning, N. M. 2002, *New Astronomy*, 7, 197
- Ramirez-Ruiz, E., MacFadyen, A. I., & Lazzati, D. 2002, *MNRAS*, 331, 197
- Ramirez-Ruiz, E., Celotti, A., & Rees, M. J. 2002, *MNRAS*, 337, 1349
- Rees, M. J. & Meszaros, P. 1994, *ApJ*, 430, L93
- Reichart D. E., 1999, *ApJ*, 521, L111
- Reichart D. E., Lamb D. Q., Fenimore E. E., Ramirez-Ruiz E., Cline T. L., Hurley K., 2001, *ApJ*, 552, 57
- Rhoads J. E., 1999, *ApJ*, 525, 737
- Rutledge, R. E. & Sako, M. 2003, *MNRAS*, 339, 600
- Sakurai A., 1960, *Comm. Pure Appl. Math.*, 13, 353
- Salmonson, J. D. & Galama, T. J. 2002, *ApJ*, 569, 682
- Sari R., Piran T., 1995, *ApJ*, 455, L143
- Tan J. C., Matzner C. D., McKee C. F., 2001, *ApJ*, 551, 946
- Thompson C., Madau P., 2000, *ApJ*, 538, 105
- Toshio M., Daisuke Y., 2000, in *Proceedings of the Tenth Workshop on General Relativity and Gravitation*, pp 373–378
- Turatto M., Suzuki T., Mazzali P. A., Benetti S., Cappellaro E., Danziger I. J., Nomoto K., Nakamura T., Young T. R., Patat F., 2000, *ApJ*, 534, L57
- Vietri M., Ghisellini G., Lazzati D., Fiore F., Stella L., 2001, *ApJ*, 550, L43
- Vietri M., Stella L., 1999, *ApJ*, 527, L43
- Wang X. Y., Dai Z. G., Lu T., 2000, *MNRAS*, 317, 170
- Whitham, G. B. 1974, *Linear and Nonlinear Waves* (New York: Wiley).
- Woosley S. E., Eastman R. G., Schmidt B. P., 1999, *ApJ*, 516, 788
- Zhang W., Fryer C. L., 2001, *ApJ*, 550, 357
- Zhang, W., Woosley, S. E., & MacFadyen, A. I. 2003, *ApJ*, 586, 356